Turbulence Measurements in a Gulf of Mexico Warm-Core Ring

Conference Paper · January 2007

DOI: 10.1115/OMAE2007-29321

5 authors, including:

Rolf G. Lueck
Rockland Scientific International, Inc.
80 PUBLICATIONS **2,616** CITATIONS
SEE PROFILE

George Forristall
Forristall Ocean Engineering, Inc.
109 PUBLICATIONS **2,462** CITATIONS
SEE PROFILE

Proceedings of OMAE07
26th International Conference on Offshore Mechanics and Arctic Engineering
June 10-15, 2007, San Diego, California

OMAE2007-29231

DRAFT

TURBULENCE MEASUREMENTS IN A GULF OF MEXICO WARM-CORE RING

Thomas M. Mitchell
Oceanographic Consulting
Houston, TX 77077

Rolf G. Lueck
Rockland Scientific International, Inc
Victoria, BC

Michael J. Vogel*
Robert E. Raye
Shell International E & P, Inc.
Houston, TX 77025

George Z. Forristall
Forristall Ocean Engineering, Inc.
Camden, ME 04843

ABSTRACT

Oceanographic measurements were made in a Loop Current Eddy in the Gulf of Mexico to characterize the turbulence associated with these eddies. Measurements were made within the eddy, and across the strong frontal boundary delineating the eddy from the surrounding waters. The survey was conducted August 23-30, 2003, from the *R/V Pelican*. The towed vehicle, the TOMI, was equipped with a special 300 kHz acoustic Doppler current profiler (*Medusa* ADCP) that had its four beams directed fore, port, starboard and down. The along-beam velocities resolved structures with wavelengths of 4 to 60 m. The vehicle also carried shear probes for measuring velocity fluctuations in the dissipation range (0.5 to 100 cycles per meter), and other environmental sensors for measuring temperature, salinity, depth and vehicle orientation. Ship equipment included a 75 and 300 kHz hull-mounted ADCP, CTD, and meteorological sensors.

Tows were conducted at 25, 50, 100 and 150 m depths around the northern edge of the Loop Eddy in currents of up to 1.7 m s^{-1}. Turbulence was detected with the shear probes, but mostly in the 130 - 150 m depth range around the local salinity maxima. The level of turbulence is weak and it is distributed intermittently in both space and time. The most energetic events of turbulence have eddy scales of at most 4 meters and velocity scales of only 1 cm s^{-1}. The typical and average values are more than 10 times smaller.

The concurrent measurements of velocity with the *Medusa* ADCP did not reveal any signals significantly larger than the noise level of this instrumentation, namely 2 cm s^{-1}. Overlap averaging of the forward directed beam reduced the noise level to 0.5 cm s^{-1} but still failed to reveal real environmental signals. This "null-result" is consistent with the simultaneous measurements taken with the shear probe. These low levels of turbulence are also consistent with reports of measurements in the Gulf Stream, the Florida Current, and a Gulf Stream Warm-Core Ring.

Funding was provided by the DeepStar oil industry research consortium. Complete details of the program are provided in Reference [6].

*Address all correspondence to this author.

PROJECT BACKGROUND

Field work was carried out using the horizontal profiling instrument TOMI (Towed Ocean Microstructure Instrument) in currents generated by an eddy in the northern reaches of the Gulf of Mexico (GoM). The purpose of this survey was to characterize the turbulence associated with these eddy features to help determine if turbulent motions within an eddy, or other high-speed current event, are responsible for undesirable low-frequency motions of oil platforms (spars). The measurements reported here were made within Eddy Sargassum, and across the strong frontal boundary delineating the eddy from surrounding waters. The target towing depths were at 25, 50, 100 and 200 meters, which are representative of the depths of spar structures. The measurement of turbulence characteristics in the flow both upstream and downstream of a spar was also a desired goal of the measurement program, however, adverse weather, time constraints and a lack of significant current around local spars during the field program rendered this objective both impossible and somewhat irrelevant. The field measurement program commenced on August 23rd, and ended August 29th of 2003, during which time over seventy-two hours of turbulence data were collected within, and around the eddy. Of this data, 25% is from depths near 25 meters, 25% is from depths near 50 meters, 35% was collected at around 100 meters and 10% is from measurements made between 150 and 200 meters. The remaining 5% of data is from periods when the instrument was on deck or at the surface. The TOMI was towed off the aft deck of the *R/V Pelican*. This research vessel is based in Cocodrie, LA.

INSTRUMENTATION

The Horizontal Profiler

The TOMI is an instrument used to measure ocean microstructure (Figure 1), and was leased for this project from the Ocean Turbulence Laboratory at the University of Victoria. The TOMI profiles horizontally, and as such is ideal for investigating the long, horizontal patches of turbulence that frequent the ocean. By

profiling within turbulent patches for extended periods, the statistical uncertainties associated with oceanic turbulence measurements are considerably reduced. The main body of the instrument is a modified fuel tank from the wing of a navy jet fighter. Within its cigar shaped outer hull reside two cylindrical inner hulls, which house a pressure case (containing the instrument's electronics), and the RD Instruments ADCP (Acoustic Doppler Current Profiler), commonly called *Medusa* (Figure 2) because of its custom transducer configuration. The pressure case in the forward compartment protrudes about 30 cm in front of the hull, and its aft two-thirds is wrapped in thick open-cell polyurethane to minimize the effect of high frequency body vibrations on the turbulence sensors mounted on the forward end of the case. The *Medusa* ADCP occupied a portion of the aft space in the vehicle, and was powered and communicated with through cabling from the forward case. The transducer cables emerged from the TOMI mid-body, connecting the internal ADCP unit to its four externally mounted transducers, which faced forwards, towards both sides, and downwards.

Fins attached at the stern of the vehicle provide stability and directionality while in tow, and two masts project 1.5 meters vertically up and 1 meter down mid-way along the body. The inclusion of masts on the TOMI allow for the spatial separation of temperature and conductivity sensors, thus providing an estimate of the vertical density gradient. Syntactic foam fills the void between the two hulls, rendering the instrument almost neutrally buoyant. A 70 kg mass is fixed to the far extremity of the lower mast to ensure the vehicle remains in the prescribed orientation during profiling, and lead plates within a center space are added to give the vehicle a slightly negative buoyancy of approximately 10 kg. The vehicle is towed by and communicates with shipboard computers through an eight conductor cable, which connects to the vehicle at a tow point near the nose. The tow cable runs forward and slightly up about 100 meters from the vehicle nose to a weighted section that acts as a damper to sudden cable movements from further up the tow line, and helps to steepen the tow cable, and hence facilitate penetration to greater depth. In this configuration, about 1000 meters of available tow cable allows the instrument to achieve depths greater than 200 meters, depending somewhat on conditions at the surface. The shipboard terminus of the tow cable is a transceiver dedicated to telemetry electronics, which is linked to both a computer that logs all data using ODAS (Ocean Data Acquisition System), and another designated to acquire the ADCP output stream only. Other machines are also employed to run software which provide a real-time visual display of certain key quantities.

The TOMI Sensors

The TOMI instrument supports a host of sensors in a variety of locations. The sensors, and quantities measured, are listed in Table 1. The sensors are, starting from the nose (Figure 1):

- Two airfoil shear probes for the measurement of the rate of dissipation of turbulent kinetic energy (ε). They were oriented to sense vertical and horizontal velocity fluctuations with scales of 0.01 to 2 meters along the direction of towing. The probes were mounted in close proximity to each other.

- Two fast-response *Thermometric* FP07 thermistors for measuring temperature (T) and its fluctuations (dT/dt). They were mounted above and below the airfoil probes.

- A set of *Sea-Bird* temperature and conductivity cells (mounted ~ 10 cm aft of the shear probes), for obtaining estimates of temperature (T) and salinity (S).

- A multi-axis inertial sensing system for measuring linear accelerations (a_x, a_y, a_z), and angular rates (ω_x, ω_y, ω_z) at the nose of the vehicle.

- A *Keller* pressure transducer (mounted on the back plate of the forward pressure case) for determining vehicle depth (P).

- Four rigidly mounted transducers looking forwards, sideways (port and starboard), and downwards (cabled to a 300 kHz ADCP), that provided velocity estimates, and the low wavenumber portion of the turbulent velocity spectrum (Φ_u, Φ_v, Φ_w). The forward looking transducer also provided estimates of the vehicle speed, U, through the water.

- Two sets of *Sea-Bird* temperature and conductivity cells mounted at the top of the upper mast and bottom of the lower mast. Concurrent measurements provided estimates of the vertical gradient of density ($\partial \rho / \partial z$), and the buoyancy frequency (N).

- Two propeller type current meters, at the top of the upper mast, and bottom of the lower mast. Their signal average was also used to estimate U, the vehicle speed.

Shipboard Instrumentation

The *R/V Pelican* has a number of oceanographic instruments that were in operation during this experiment. The first of these instruments is the CTD (Conductivity, Temperature, Depth instrument), which provided "snapshots" of ambient temperature and salinity profiles of water masses from within and outside of the eddy. Data from the CTD also proved to be very useful for confirming our position relative to the eddy.

Also present in the hull of the *R/V Pelican* were two downwards looking ADCPs (75 kHz and 300 kHz), which were primarily used to observe profiles of current strength and direction under the vessel. These velocity profiles were an effective means to know which part of the eddy was being sampled.

The vessel's flow-through MIDAS system provided continuous sampling of sea surface temperature, conductivity, chlorophyll fluorescence, and transmissometry. MIDAS also integrated information from the ship's meteorological suite into the data set. The meteorological suite consists of a wind monitor, a barometric pressure sensor, and a temperature and relative humidity sensor.

MEASUREMENT PROGRAM

Overview

This experiment was conducted as a result of the adverse effects that warm-core rings appear to have on spars. These energetic warm core rings or "eddies", whose largest dimension can vary from 200 to 400 kilometers, stem from instability processes in the Gulf Stream Loop Current. Accompanying these large, anti-cyclonic eddies, are smaller warm core rings, as well as a variety of cyclones (cold core or cyclonic frontal eddies) that are also a result of instabilities in the Loop Current. These smaller eddies tend to have diameters of 50 km or less. In this paper, the vertical co-ordinate is expressed in units of m to indicate the depth with respect to the mean free surface. The unit of dBar (decibars) is used to indicate pressure.

Figure 3 shows the ship's track as it transited from port through a small cyclonic eddy (1) – (2), then entered the main body

of Eddy Sargassum at (3). The weather grew progressively worse over the measurement period. The first few days were calm and clear, which were ideal for the ballasting and initial testing period. Figure 4 is a plot of true wind speed and wind direction from the measurement period. The wind speed shown in the upper panel remained relatively low (< 15 knots) during the first few days of towing (Aug. 24-27), and with the exception of the 24th, came primarily from the south or SE. Wind direction switched abruptly midday on the 27th to the NE, with associated light breezes (< 10 knots), and then switched to southerlies again by late evening. Over the course of the remaining three days of surveying, the wind was consistently from the SSE, and became progressively stronger because of a tropical storm approaching from the southeast. By the 29th, winds were consistently higher than 20 knots, and launching and recovery of the towed vehicle became progressively more difficult. Mean wind speed during the experiment was 10.3 knots, and was primarily from the SE (132.6°). The sea state was calm (light chop) for the first number of days, with a noticeable change to growing swell by the 28th. The steady south-easterly winds coupled with significant fetch enhanced swell height such that by the afternoon of the 29th, swell height exceeded 10 feet. Overall, the conditions during the measurement period were ideal, and only became an issue at the end of the survey during the final recovery of the instrument.

CTD casts were made along the track line shown in the inset of Figure 5. The initial plan had been to use the imaginary line between these stations as a survey track for the towed vehicle, however, ship maneuverability in lateral currents and tow speed limitations forced the ship off this line during most tows. The eddy current drove the ship downstream (eastward) in each case, and as a result time was lost returning to the CTD line. Tows were initially planned to be from the NW to the SE, or from SE to NW, across the front generated by the eddy. In reality, tows tended to be towards the NE and SE.

Tow Descriptions

Initial testing of the TOMI system was conducted in the morning of August 23rd. The system was ballasted, and some initial problems with the PIO board of the *Medusa* ADCP were solved by replacing the board with a spare board. The TOMI was ready to begin the first survey by mid-morning on August 25. Some problems occurred from time to time during the tows, and are briefly described in the following sections.

Tow Pattern Overview. A composite of all tows is shown in Figure 6 where the lines have been color coded to reveal the depth of the towed vehicle. Tow information is summarized in Table 2. Virtually all towing was conducted within the eddy. Tow 1 crossed the predicted eddy front twice while Tow 4 reversed direction at the front. The individual tow tracks are detailed in Figure 7, showing both the geographic position and the depth of the vehicle. The position and depth lines have been color coded according to time so that position can be correlated with depth.

Tow 1. The first tow of the survey (Figure 7, top) spanned over 24 hours, and commenced on the evening of Aug. 25 (Table 3). The *R/V Pelican* was well within the eddy, and the initial track line was NNW. The instrument was equilibrated at a depth of approximately 27 meters, near the first target depth of the survey. The tow continued northwards for some hours, with a heading change to the NW to improve ship maneuverability through the eddy front. The ADCP appeared to be functioning well out to bin 30 (30 meters), beyond which the signal intensities were low and velocity estimates consistently bad. A check on the velocity profile from the ship's 75 kHz ADCP confirmed that we were in the eddy. The current was traveling at 1-1.5 ms^{-1} towards the NE, and penetrated to a depth of at least 150 meters. In the early hours of August 26, the Pelican crossed the eddy front, and re-entered the eddy heading SE. Besides a tendency for the port looking transducer (T#2) to under-perform (errors in the last 4-5 bins) relative to the other transducers, all systems were functioning reasonably well. At 07:43 CDT the ADCP cell width was reconfigured to 4 meters in an attempt to improve velocity estimates in the outer bins. This change caused the ODAS system to have difficulty in logging the ADCP serial stream. At 09:30 CDT, the instrument was repositioned to a depth of 50 meters, where it remained for the next 9 hours. At 12:27 CDT, the serial buffer size was increased, and soon afterwards the ADCP cell width was dropped to 2 meters to improve resolution. At 18:30 CDT, 800 meters of tow cable was payed out, such that by 19:15 the instrument was vertically stable at 145-150 meters, moving at 1.2 ms^{-1}. The instrument was recovered by 21:50 (see Figure 7).

Tow 2. Before the TOMI was deployed for the second tow, a number of changes were made to its configuration. Weight was removed from the tail to correct a slightly nose up (7°) attitude observed during Tow 1. A radio transmitter was removed from the upper mast, and transducer cables at the ADCP unit were also interchanged as a diagnostic tool.

Initially, the plan had been to start the tows at various depths from the same geographical location, however, the strong currents generated by the eddy had relocated the *R/V Pelican* far to the east from that point over the course of the first tow. Hence, a decision was made to carry on with the survey, under the assumption that the characteristics of such a large eddy were unlikely to change significantly from regions separated by a few dozen nautical miles. TOMI was deployed at 00:35 CDT on August 27. The instrument dived to 100 meters within the first 30 minutes of the tow, and remained at approximately that depth until recovery 10.5 hours later. Once again, the tow commenced from a position within the eddy, albeit further to the east, with a planned northerly tow track. In an attempt to remain in the vicinity of the CTD stations to the west, the ship headed to the NW in order to progress northwards in the north-easterly moving current.

During this tow, the *Sea-Bird* conductivity probe at the base of the lower mast on the TOMI malfunctioned, and the downwards-looking transducer (previously port facing) was still under-performing. The weak signal was clearly identified as a problem in the internal electronics of the ADCP. Tow 2 was terminated at 11:07 CDT.

Tow 3. The signal strength problem was solved by exchanging the DSP board in the *Medusa* with the board from a backup unit. At 16:14 CDT, TOMI was launched near the north edge of the eddy front, heading SSE. After 30 minutes at a depth of 20 to 30 meters, most of the tow cable was payed out with the intention of reaching 200 meters depth. The TOMI was recovered at 19:50 CDT so that the *R/V Pelican* could steam to the Tow 4 start location.

Tow 4. The *R/V Pelican* arrived in the vicinity of CTD Station 3, and the TOMI was deployed in the early hours of Aug. 28. The characteristic velocity profile of the eddy was present, and towing commenced in the direction of the eddy front to the NNE. At 03:30 CDT, 45 minutes into the tow, the tow cable was run out to the 800 meter mark, and the instrument dropped rapidly to 200 meters, only to rise again to 150 meters as a result of increased speeds due to downwind travel. At 04:30, the TOMI had climbed to 140 meters, so the ship speed was slowed as much as possible. The vehicle speed then dropped to 1.2 ms^{-1}, and the vehicle settled down to an average depth of 175 meters. Unfortunately, these greater depths proved difficult to maintain due to the deteriorating conditions at the surface, such that by 06:00 the instrument had once again risen to 130 meters. Soon after 07:00, it was observed that the tow cable angle was 60°, so the ship was forced to turn to port (heading north) to correct for this. The speed of the ship coupled with lateral currents, caused the

instrument to rise to a depth of 95-105 meters during this period. The instrument then underwent a rapid climb to approximately 40 meters as it passed through the eddy front, followed by a rapid descent to 80 meters when the ship turned to the SE, and then back up to a depth of 25 meters as the vehicle began to pick up speed again. The intention was to re-enter the eddy front for this final leg of the tow at 25 meters, however, the surface current carried the *R/V Pelican* eastward (current direction 80°), and away from the front, prompting a recovery at 11:45 CDT. The recovery proved to be more difficult than anticipated due to the swells generated by winds from the south, and the upper current meter experienced some minor damage after brushing against the side of the ship.

Tow 5. The *R/V Pelican* steamed for 3 hours SW from the recovery location to arrive in the vicinity of CTD Station 3 at 15:00 CDT. CTD Cast 13 was made, and the towed body was deployed. The ship headed north, over an eddy current of 1.2 ms^{-1} heading east, resulting in a track towards the NE. By 22:00, the instrument had passed through the eddy front, and the *R/V Pelican* was turned to a heading of due south. The instrument dropped to a depth of 130 meters on the turn, but otherwise remained at a depth of 50 meters for the first 6 hours of the tow. At 02:00 on the morning of Aug. 29, the instrument was dropped to a target depth of 100 meters, and was maintained within the 90-110 m depth range for the next 9 hours of towing. At 12:30, the ship was turned around, and tracked towards the NNE with TOMI at 155-165 meters depth. As the afternoon progressed, a number of unexplained ODAS software crashes combined with deteriorating conditions (8-10 ft swell) began to make the recovery of the instrument a growing priority. However, the existence of a shear layer at 160 meters that had been present for a number of hours that afternoon persisted, and the survey was continued at that depth. The microstructure turbulence was quite pronounced at times, and yet was not accompanied by any ADCP signals above the noise level. At 17:30, the final recovery took place near the northern edge of the eddy.

DATA ANALYSIS

Turbulence Data

Dissipation of Turbulent Kinetic Energy (ε). Under the assumption of local isotropy of the turbulence, the rate of dissipation of turbulent kinetic energy is determined by

$$\varepsilon = 7.5\,\nu\,(\partial w/\partial x)^2 \quad \text{or} \quad 7.5\,\nu\,(\partial v/\partial x)^2 \quad [\mathrm{W\,kg^{-1}}] \qquad (1)$$

where ν is the kinematic viscosity ($\nu \sim 1\times10^{-6}$ m^2 s^{-1}), $\partial w/\partial x$ and $\partial v/\partial x$ are the shears of vertical and athwartship velocity fluctuations with respect to the direction of towing, respectively, and the bold font in (1) indicates a spatial average along the direction of towing [2]. Most of the variance of shear resides at scales shorter than 1 m. The shear probe (at front of the towed body, Figure 1; Figure 8) can resolve velocity fluctuations with wavelengths as short as 0.01 m. The largest scales that can be resolved with the shear probe is determined mainly by the length and stability of the platform holding the probes, namely a few meters for the towed vehicle *TOMI*. In practice, the variance of shear [$(\partial w/\partial x)^2$ or $(\partial v/\partial x)^2$] is obtained by integrating the shear spectrum in wavenumber space from 1 cpm to an upper limit that depends on the signal-to-noise ratio of the measurements. The upper limit is never less than 10 cpm and never more than 100 cpm. The unit of "cpm" is cycles per meter, and is numerically the inverse of the wavelength. Wavenumber is a spatial "frequency". For example, a spatial structure with a wavenumber of 10 cpm undulates through 10 cycles over a distance of 1 m. Isotropy at dissipation scales is assumed by (1) but there is no requirement for isotropy at the larger, energy-containing, scales. In fact, anisotropy must exist at some scale for there to be stress in the fluid and, hence, shear-driven turbulence.

The dissipation of turbulent kinetic energy is the rate at which the energy of turbulent motions is removed by molecular friction, and occurs only once the turbulence has cascaded down to small enough scales for viscosity to be effective, that is, the 0.01 – –1 m range. It is the ultimate sink for turbulent kinetic energy, and gives a measure of the rate of transfer of energy through a flow field. This transfer is from the large-scale "mean" flow, such as the Loop Current Eddy, through instabilities and over-turns down to the centimeter size dissipation scales where the energy is removed by molecular viscosity in a thermodynamically irreversible fashion. Coastal regions can have levels for ε up to 10^{-2} W kg^{-1}, but typically in the open ocean and at depth, levels for ε are many decades lower. The examples of shear spectra shown in Figs. 20 and 21 have corresponding dissipation rates of $\varepsilon = 3\times10^{-10}$ W kg^{-1} (4h) and 5×10^{-8} W kg^{-1} (6.43h) for the spectra from Tow 2, and$\varepsilon = 2\times10^{-6}$ W kg^{-1} (4.1h) and 3×10^{-10} W kg^{-1} (6.7h) for the spectra from Tow 4.

Engineers may be more comfortable with characterizing turbulence in terms of rootmean-square (rms) velocity fluctuations relative to some typical flow velocity (turbulence intensity), rather than in terms of the rate of dissipation. This is not the usual practice in oceanography because turbulence will occur even when there is no mean velocity. The energy for turbulence frequently comes from internal waves which impart no mean velocity to the fluid but do induce considerable shear. In fact, the shear can be strong enough to overcome the stabilizing effect of density stratification and (literally) overturn the water locally to create turbulent motions. The resulting velocity fluctuations are related to the rate of dissipation by

$$\varepsilon = w^3/l \qquad (2)$$

where l is the typical length scale of the fluctuations and w is the rms vertical velocity. The rms horizontal velocity fluctuations will be of the same order of magnitude, but as much as 2 or 3 times larger because of density stratification. This is discussed further later in this section. It is important to note here that the ocean is usually a very low-turbulence environment from an engineering perspective. Away from boundaries, the length scale of turbulent fluctuations is seldom more than 1 m, and the velocity fluctuations, inferred from (2), seldom exceeds 0.01 m s^{-1}. This seems to be true even in strong ocean currents such as the Gulf Stream. Consequently, the "intensity" of turbulence in a strong current is less than 1%. Wind- and water-tunnel designers would be very proud to claim such low levels of turbulence for their products. The major objective of this project was to test whether, or not, this is also true for Loop Current Eddies in the Gulf of Mexico.

Shear Spectra. The horizontal and vertical velocity components associated with small-scale turbulence were measured with single-axis airfoil probes (Figure 8). The probe is a pointed body of revolution which utilizes hydrodynamic lift force to measure one cross-stream component of velocity. The charge generated by the sensor's piezo-ceramic beam is passed through a charge-transfer amplifier, and then through a differentiating circuit to improve the signal-to-noise ratio at higher frequencies. In the presence of a constant speed through the water, this differentiated signal becomes a measure of the along-stream gradient of cross-stream velocity fluctuations. The probe is mounted so that its mean travel velocity (U) through the water is aligned with the axis of revolution of the probe, and the measured signal is the fluctuating flow (w or v) orthogonal to this direction of travel.

Instantaneous values for microstructure shear ($\partial w/\partial x$ and/or $\partial v/\partial x$) are obtained from the probe signal by applying the Taylor frozen field assumption

$$\partial / \partial x = 1/U(\partial / \partial t) \quad (3)$$

to the differentiated voltage generated by the probe.

Figure 9 has been included to help with the interpretation of turbulent shear spectra measured with the shear probes. These curves represent the theoretical (ideal) shear spectrum for dissipation rates of $\varepsilon = 1 \times 10^{-10}$ to 1×10^{-4} W kg^{-1} [4]. The important features to note are the shapes of the spectra, and the spectral levels associated with the different rates of dissipation. An easy reference when looking at spectra is the wavenumber (cycles per meter) location and level of the spectral peak.

Two examples of shear spectra with respect to wavenumber from Tow 4 are shown in Figure 10, and represent regions of lower and higher turbulent shear. For these two examples, the spectral levels from Probes 1 (vertical fluctuations) and 2 (horizontal fluctuations) agree over all wavenumbers. The upper panel shows the elevated shear levels found at hour 4.1, and the lower panel exhibits spectra for weaker shear levels (6.7h). Comparison of the curves in the upper panel with the theoretical spectra in Figure 9 suggest that these spectra are from a region where $\varepsilon \approx 1 \times 10^{-6}$ W kg^{-1}. Integrating these spectra in wavenumber space gives the actual rate of dissipation, $\varepsilon = 2 \times 10^{-6}$ W kg^{-1}.

A very compact way to view spectra from an entire tow is to plot them as images, where color indicates spectral value. Figure 11 shows two color images of shear spectra generated from measurements made by airfoil probes during Tow 4. For both panels, frequency (Hz) and instrument depth (dBar) are indicated on the y-axis, and time of day (CDT) is on the x-axis. Each vertical line is a spectrum of 32 seconds of shear data, and the color bar on the right links the image colors to spectral levels. This somewhat unconventional method for plotting shear spectra is also useful for identifying signal contamination relative to frequency. For example, lines at 120, 180 and 240 Hz identify power line noise. There is also a blue-green band at approximately 160 Hz, and a number of thin bluish bands below 50 Hz that are caused by vehicular vibrations. Most contamination is quite small, and is only visible in the images because of the logarithmic color axis. When compared to the depth profile, we see that the strongly turbulent regions coincide with 130 - 150 meters depth, which happens to be the depth of the salinity maxima. In the vicinity of hour 4, spectral levels are slightly larger than 10^{-3} s^{-2} cpm^{-1} in the 10 – 70 Hz range, which implies that dissipation rates in that region are equivalent to, or slightly above, 10^{-6} W kg^{-1}. Hours 6 to 8 represent some of the lowest levels of shear measured during Tow 4, and comparison with the ideal curves suggest that the dissipation rate for these measurements is approximately 10^{-10} W kg^{-1}. In fact, the shear levels are so low in this region that a good deal of the signal is likely noise. The individual spectra shown in the lower panel of Figure 10 come from this region, and are a good example of the limit for shear measurements with our instrument. The lowest wavenumbers (1 - 10 cpm) appear to be contaminated, and as a result the curve bulges in this range. The spectra at 10 cpm imply a dissipation rate just above 10^{-10} W kg^{-1}, and levels at higher wavenumbers are fairly constant, suggesting the noise floor has been reached. These spectra, when integrated in wavenumber space, produce $\varepsilon = 3 \times 10^{-10}$ W kg^{-1}. This value for ε is considered the noise level of the TOMI.

Signal contamination stemming from vehicle vibrations is also a necessary consideration when using shear spectra to estimate turbulence levels. A series of signal processing steps were taken to remove vehicle vibrations from shear probe signals, to ensure that estimates of the rate of dissipation are not biased by motion contamination. The first step was the application of a de-spiking algorithm to the raw shear probe data, which removed data spikes stemming from impacts with plankton. These impact spikes are easily identified and replaced by the local mean. Spikes tend to constitute only a small fraction of the shear data (0.01 %). A section of data with strong vibrations was then selected to determine the transfer function relating Az and Ay, to shear probe signals. The coherent noise in the shear signals was then removed with Weiner filters.

Buoyancy Frequency (N). The buoyancy frequency (N) is a primary measure of stability in a stratified fluid. Unfortunately, because N involves estimating the vertical gradient of density, it is not necessarily an easy parameter to measure from a near horizontal measurement path. The Brunt-Vaisala frequency (N^2) is

$$N^2 = g[\alpha(\partial T/\partial z + \gamma) - \beta(\partial S/\partial z)] \quad [\text{rad}^2\text{s}^{-2}] \quad (4)$$

where $\partial T/\partial z$ and $\partial S/\partial z$ are the vertical gradients of temperature and salinity respectively, $\alpha = -\rho^{-1}\ \partial\rho/\partial T$ is the thermal expansion coefficient, $\beta = \rho^{-1}\ \partial\rho/\partial S$ is the contraction coefficient for salinity, and γ is the adiabatic lapse rate. To provide estimates of N, vertically separated concurrent measurements of temperature and conductivity were made using the *Sea-Bird* sensors on the nose and masts of the vehicle.

Ozmidov Length Scale (L_o). The Ozmidov length scale

$$L_o \equiv (\varepsilon/N^3)^{1/2} \quad (5)$$

is the longest vertical overturning length scale permitted by the ambient stratification. This length scale is determined from the kinetic energy available for overturning motions (which is proportional to ε), and the potential energy of stratification suppressing vertical motions (which is proportional to $L_o^2 N^3$). For a given stratification N, the overturning scale of turbulent eddies increases with increasing dissipation rate as $\varepsilon^{1/2}$. For a given dissipation rate ε, the length scale of eddies decreases with increasing stratification as $N^{-3/2}$. As N goes to zero, which it may in the surface mixing layer, L_o becomes meaningless, and hence L_o is really only useful for estimating the size of turbulent scales in regions that are stably stratified ($N > 0$). Some of the larger overturning scales shown later are from the surface mixing layer, where the stratification is very small and L_o is not a good indicator of eddy size. Almost all tows were made in stratified water, but care should be used when interpreting length scales for the shallow sections of the tows.

Comparing ε, N and L_o. Figure 12 depicts the variations, along the tow path, of the rate of dissipation (ε), the buoyancy frequency (N), the Ozmidov length scale (L_o), the vehicle depth and the local current speed for Tow 4. Similar plots were prepared for the other tows, and are presented in Reference [6]. As discussed in the next section, the highest turbulence levels were measured in Tow 4, so detailed shear probe data are included only for Tow 4.

We plot twice the Ozmidov length scale because of the following physical interpretation of eddy structure. If we imagine eddies to be rotating cylinders of water, then turbulent fields are made up of many of these cylinders. The smallest structural denomination in this field is a repeating cycle consisting of two counter rotating cylinders, and hence the effective size of turbulent overturns is perhaps better described by $2 \times L_o$.

One general observation is that turbulence levels were relatively low within the eddy, and at the eddy front, for the majority of the measurement period. Typically, dissipation rates were lower than $\varepsilon = 10^{-8}$ W kg^{-1}, and were only intermittently above 10^{-7} for a few hours in Tow 4 for regions below 130 meters depth, and a few hours at the very end of Tow 5 for a similar depth. Shear probe data from 0 - 10 meters depth have not been included in the estimates for ε because ship wake reaches 5 - 6 meters depth. The value for N over the course of the 5 tows was typically greater than 1×10^{-2} s^{-1}. The buoyancy frequency came close to zero for a short period at the beginning of Tow 1, and periodically during Tows 3, 4 and 5, but for the most part the water column in the survey region was stably

stratified. Some of the lower values for N coincide with towing in the surface mixing layer. However, other instances where $N \sim 0$ are found at much greater depth ($P > 100$ m), and these show that mixing and turbulence are definitely occurring far below the surface. Two examples of mixing at depth can be seen for hours 4.7 and 6.4 from Tow 4 (Figure 12). The overturning length scales in these regions was as large as 4 meters.

The following description is an assessment of the dissipation rate, buoyancy frequency and the estimated size of turbulent scales expected for the tows carried out during the measurement program. During Tow 1, moderately low values for the dissipation rate, and strong stratification yielded overturns rarely larger than 0.5 meters at 25 meters depth, with the occasional instantaneous value exceeding 1 meter. Estimates of $2 \times L_o$ later in the tow (at 50 meters depth) rarely exceeded 0.3 meters in size. Similarly, $2 \times L_o$ values from Tow 2 (at 100 meters depth) rarely exceeded 0.3 meters, and in fact were generally lower than 0.1 m. The 4 hours of Tow 3, which we thought was being conducted outside of the eddy, yielded moderately low dissipation rates ($\varepsilon < 10^{-7}$ W kg^{-1}). Values for $2 \times L_o$ were less than 0.3 meters for most of the tow, except for the first hour where lower values of N allowed for the occasional value of $2 \times L_o$ to exceed a meter. Higher values for the dissipation rate at the beginning of Tow 4, where ε occasionally exceeded 10^{-6} W kg^{-1}, resulted in relatively higher estimates of $2 \times L_o$. Values were intermittently above 1 meter at the beginning of the tow, occasionally exceeded 2 meters, but were typically smaller than 0.5 meters. These higher dissipation rates during Tow 4 corresponded with deeper towing (130 - 200 meters), and once the vehicle was brought to shallower depths later in the tow, values for ε decreased, as did estimates for $2 \times L_o$. Lower dissipation rates during the majority of Tow 5 kept the estimates for $2 \times L_o$ typically smaller than 0.3 meters, with the exception of four instances where $2 \times L_o$ exceeded 4 meters. A descent to 175 meters towards the end of the tow yielded higher than average values for ε and a broader range in $2 \times L_o$ values ($0.1 \leq 2 \times L_o \leq 1.5$).

The measurement of the rate of dissipation of turbulent kinetic energy using shear probes, and of the buoyancy frequency using *Sea-Bird* CT sensors, indicates that there are intermittent regions of strong turbulence with scales ~ 4 meters, but that the vast majority of the water has extremely low levels of turbulence with overturning scales shorter than 1 meter. This finding is consistent with other measurements reported in the scientific literature, which indicate that open ocean turbulence is weak, mixing lengths are generally less than 1 meter, and that turbulence occurs intermittently in space and time. This is even true in western boundary currents [1], and Gulf Stream warm-core rings [3]. Turbulence, when it does occur, is usually associated with interleaving (such as maybe occurs around the salinity maximum in the Loop Eddy), and at doubly-diffusive interfaces. However, all findings to date indicate that even the more intense occurrences of ocean turbulence below the surface mixing layer have eddy scales that are less than or equal to about 1 meter, and that the velocity fluctuations associated with these eddies are rarely larger than a centimeter or two per second.

ADCP Data

Overview. As mentioned in the earlier section dedicated to tow descriptions, the *Medusa* ADCP had some problems with signal quality during Tows 1 and 2. Thus, ADCP data were processed only from Tows 3, 4 and 5.

In this section, we concentrate on Tow 4 because the measurements taken with the shear probes indicate that this tow had the largest turbulence at dissipation scales. The detection of oceanic turbulence with the *Medusa* ADCP is, therefore, most likely to occur in Tow 4.

We present the alongbeam de-trended profiles (which removes vehicular motions from the measurements) for all 4 beams. For the forward directed beam, it is possible to average many pings because water ahead of the towed vehicle is sampled many times by the approaching vehicle. We call this the "over-lap averaged" velocity because successive pings over-lap except for a small amount due to the displacement of the vehicle between pings. The measurement noise standard deviation is reduced four-fold (or more) by this over-lap averaging. Finally, we compute the wavenumber spectra of the velocity fluctuations along each beam to decipher the structure of the turbulence.

Readers familiar with standard ADCP configurations may wonder how the *Medusa* data are corrected for the motion of the towed vehicle that carried the *Medusa* system. Because of the unorthodox configuration of the transducers, very little correction is needed. For example, the *Medusa* was not used to measure the horizontal velocity vector. Instead, it was used to measure the velocity of the water in the direction of each sound beam as a function of distance along that beam of sound. The variations along each beam represent spatial flow structures (i.e. turbulence) as well as noise and intrinsic instrument bias. The 4 beams were directed forward, to port, to starboard and downward. The motion of the vehicle along the direction of a beam adds vectorially to the measurement of velocity along that beam. This addition is independent of range (or distance along the beam). Vehicular motion adds a range-independent bias to the velocity measurements along a beam and this vehicle-induced bias is simply removed by subtracting the range-averaged (or bin-averaged) velocity from each bin. For example, the forward directed beam will be strongly biased by the speed of the vehicle through the water. The average velocity in the forward beam (out to a range that gives reliable measurements) represents the forward velocity of the towed vehicle. The other transducers are oriented to be nominally orthogonal to the direction of towing and, so, should contain no contribution from the forward motion of the vehicle. However, the transducers are not perfectly orthogonal and the small pitch and yaw of the vehicle induces a small fraction of the forward speed into these nominally orthogonal transducers. After some experimentation we decided to linearly de-trend the data along each beam, for each ping, rather than subtract a single value.

De-trended Velocity. The velocity signals reported back to the ADCP are a combination of vehicle velocity, oceanic signals, and instrument bias and noise. The mean velocity and range dependent bias for each beam (forwards, sideways and downwards) is determined by fitting a polynomial to the range 0 to 60 for each transducer. The data from bins beyond 60 meters were ignored, because they are either bad or clearly biased. The algorithm used to de-trend the ADCP data performed a ping by ping linear fit to the data from each transducer, and then subtracted this fit from the raw values to yield "residual" velocity estimates, hereafter referred to as the de-trended velocities. This linear de-trending of the velocity bins between 0 and 60 m range automatically removes vehicular motions (which are range independent), range dependent instrument bias, as well as real oceanic structures with scales longer than the maximum range of 60 m. Details of this procedure and other processing techniques are presented in Reference [6].

Figure 13 shows the de-trended version of the data from all four *Medusa* ADCP transducers. The top panel incorporates velocity estimates from both sideways looking beams, the middle panel shows estimates from the forward beam, and the lower panel displays estimates from the downwards looking beam. The time of day is on the y axis, and the distance away from the transducer (range) is on the x axis. The bar to the right of each panel gives the velocity scale in mm s^{-1}, and further to the right still are plots of the instrument depth (P), and pitch angle. The pitch is the angle between the axis of the instrument and the horizontal, and is multiplied by 10 on this plot simply to make it visible using the same scale as P. These de-trended velocities are remarkably small; during this tow the velocity signals

seldom exceed 2 cm s^{-1} for bins in the range 0 - 60 meters. The *Medusa* velocity measurements appear to be at the noise limit of the instrumentation.

The top panel in Figure 14 once again displays the de-trended velocities from the forward looking transducer (Tow 4), with time on the y-axis, and distance from the transducer on the x-axis. The middle panel is a plot of velocity spectra with respect to wavenumber, where time is on the y-axis, wavenumber is on the x-axis, and spectral level is represented by colors referenced to the color bar on the right. The wavenumber range shown is approximately 0.01 to 0.25 cycles per meter (cpm), and the spectral range is 1 to 5 $mm^2\ s^{-2}cpm^{-1}$. These spectral estimates were generated using de-trended velocity estimates out to 60 meters, so as to avoid spectral contamination from the bias in the outermost bins. The velocity bias in the 30 to 50 meter range previously discussed for the forward looking beam appears as significant low wavenumber content ($0.01 < k < 0.03$) in the spectral estimates up until just after hour 4. This low wavenumber content returns again halfway through hour 9, and remains for the duration of the tow, again likely the result of an instrument bias. The bottom panel in Figure 14 is a plot of two separate spectra, the first generated from velocity estimates acquired between hour 4 to 4.25, and the second from hour 6.5 to 6.75. The first spectrum (blue) represents velocity data from a region encompassing the midrange bias, and the second (green) is generated from velocity estimates not exhibiting this feature. The effect of this bias is clearly seen in the difference in low wavenumber content between the two spectra. The area under the second spectrum provides a variance estimate of $\sigma^2 = 250\ mm^2\ s^{-2}$, and a standard deviation of $\sigma = 15.8$ mm s^{-1} (6.5-6.75h). This estimate of the standard deviation is approximately equal to the measurement noise predicted by RD Instruments.

The top panel in Figure 15 displays the de-trended velocities from the starboard looking transducer for Tow 4. As with the forward beam, the plot of starboard velocity exhibits the instrument bias in the outer bins, and has larger than average velocities at the beginning of the tow due to side lobe reflection off the surface. Besides these features, very little velocity structure is present, and values lie in the limited range of ±2 cm s^{-1}. The middle panel is a plot of starboard looking velocity spectra with respect to wavenumber, and the bottom panel shows two spectra for the same time periods (4 to 4.25h, and 6.5 to 6.75h) plotted in Figure 14. The side lobe noise at the beginning of the tow manifests itself as higher spectral values at lower wavenumbers. The two average spectra in the bottom panel show slightly different levels with respect to wavenumber, and produce standard deviations of approximately σ = 15.0 mm s^{-1} (blue) and $\sigma = 12.3$ mm s^{-1} (green). This second value for standard deviation, when compared to its counterpart determined from the forward beam ($\sigma = 15.8$ mm s^{-1}), provides a measure of how different transducers interpret the same turbulence. In fact, the lack of turbulent structures and the generally low velocity estimates suggest that, for the most part, the ADCP velocity estimates are primarily instrument noise. The difference in σ based on forward looking and starboard looking velocity data is then perhaps more a measure of the different noise levels associated with these transducers.

Overlap-Averaging. Figure 16 demonstrates the improvement in signal-to-noise achieved through overlap-averaging of successive pings. Overlap-averaging is the name given to a technique that sorts ADCP data in space through interpolation. The ping data are interpolated onto a uniform grid in the direction of travel and give a position according to the actual position of the vehicle and the range of the bins. For the speed of towing and the range of the forward beam, approximately 19 pings can be averaged at a given range, which vastly improves the statistical reliability of the velocity estimates.

The top panel in Figure 15 shows the de-trended velocity estimates for hours 4 to 5 from Tow 4, while the middle panel shows the same data after overlap-averaging. The lower panel in Figure 16 shows the mean and standard deviation of these velocity profiles as a function of range. The standard deviation for the de-trended velocities is just under $\sigma = 2$ cm s^{-1} out to 60 meter range, whereas σ is approximately 0.5 cm s^{-1} in the same range after overlap averaging is applied to the de-trended data. The clearly negative trend visible in the outer bins for both velocity means once again indicates that a bias exists in all velocity data in bins beyond 55 meter range. The previously discussed mid-range bias ("crowning") at 30 - 50 meters is clearly visible throughout hours 4 - 5.

The lower panel in Figure 17 shows the standard deviation of individual pings for the range 0 - 60 meters. For the de-trended data, the standard deviation is fairly steady over the one hour interval, and is approximately $\sigma = 2$ cm s^{-1}. For overlap-averaging, $\sigma = 0.5$ cm s^{-1}. Figure 16 gives the standard deviation as a function of range, and Figure 17 gives the standard deviation as a function of time, and both give a value of $\sigma = 2$ cm s^{-1}, which is slightly below the value predicted by the manufacturer. Overlap-averaging gives standard deviations, for both methods, that are four times smaller, which is almost exactly the value expected when averaging noise. A true environmental velocity signal would not have been attenuated by overlap-averaging.

The overlap-averaged versions of the raw and de-trended data from the forward beam (Tow 4) are shown in Figure 18. The raw data consists primarily of the travel velocity signal, and comparison with the depth profile on the right shows a correlation between vehicle speed and vehicle orientation. Vehicle speed tends to decrease to below 1 m s^{-1} as the vehicle drops to depth, and occasionally exceeds 2 m s^{-1} during climbs to shallower depths. Little information about velocities due to turbulence can be discerned by viewing raw data from the forward beam, since these values are orders of magnitude smaller than the travel velocity. The lack of significant turbulent structures becomes more evident when we compare the raw data to its de-trended version in the lower panel. With travel velocity removed, we see that for the vast majority of the tow, turbulent velocities are so small that they remain indistinguishable from noise. In fact, the only features which appear in the operating range of the instrument are biases that have nothing to do with the physical environment.

The effect of overlap-averaging on wavenumber spectra is demonstrated in Figure 19. The top panel shows the overlap-averaged de-trended velocity estimates from the forward looking beam (Tow 4), and the middle panel is a plot of its associated spectra with respect to wavenumber. The spectra, not surprisingly, continue to exhibit significant energy at low wavenumber during the first few hours of the tow as a result of the mid-range instrument bias (crowning). The lower panel shows the spectra from the overlap-averaged data for the same two examples shown in Figure 14. Those previous examples were calculated using de-trended data and, as a result, were contaminated to a greater degree by noise. The improvement in signal-to-noise from overlap-averaging produces spectral levels below those based on de-trended data, which suggests that in general for this tow, the signal strength rarely exceeds the noise level. A quick calculation of variance based on the area under the curves yields standard deviations of $\sigma = 7.9$ mm s^{-1} for hour 4 to 4.25, and $\sigma = 3.2$ mm s^{-1} for hour 6.5 to 6.75. The estimate for σ from the de-trended data for hour 6.5 to 6.75 is $\sigma = 15.8$ mm s^{-1}, which is 5 times larger. This reduction in standard deviation, and the attenuation of the spectra with increasing wavenumber, is exactly what is expected from averaging noise. Therefore, it is likely that the actual environmental velocity fluctuations are still smaller than 3 mm s^{-1}!

Comparing Velocity and Dissipation Rate Estimates. A simple

relationship that ties the rate of dissipation of turbulent kinetic energy to the velocity scale of the turbulent overturns is described by

$$\varepsilon = u^3/l \quad (6)$$

where u is the turbulent velocity, and l is the size of the overturn. The spectrum for hour 4 - 4.25 (Tow 4) shown in the lower panel of Figure 19 has a dissipation rate of $\varepsilon = 1 \times 10^{-6}$ W kg^{-1}, and an average length scale $2 \times L_o \sim 1$ meter (Figure 12, lower panel). By rearranging (6) we can estimate the magnitude of velocity associated with these turbulent scales, where

$$u \sim (\varepsilon \times 2 \times L_o)^{1/3} \sim (1 \times 10^{-6} \times 1)^{1/3} \sim 10^{-2} \text{ m s}^{-1} \quad (7)$$

The calculation of standard deviation based on integrating the spectrum in wavenumber space yielded $\sigma = 7.9$ mm s^{-1}, which agrees well with the estimated velocity calculated in (7) for 1 meter overturns. Thus, even for one of the more turbulent regions detected by the shear probe, the stratification inhibited the scale of overturns to 1 meter and the velocity fluctuations are approximately 1 cm s^{-1}, and barely detectable with the ADCP, even after overlap-averaging.

Time-space series plots (not included) from Tow 3 and Tow 5 were prepared (similar to Figs. 30-34, except without spectra plots). The results are similar to those shown for Tow 4. The de-trended velocities are typically in the range of ±2 cm s^{-1} with only a few rare occasions when the magnitude reaches 4 cm s^{-1}. The overlap-averaged velocity estimates are much smaller than were found for Tow 4. For Tow 5, in the range of 0 to 40 m, the velocity fluctuations are within less than ±1 cm s^{-1} **continuously for 16 hours**! There simply is no environmental velocity signal that can be detected with acoustic techniques. Only the ultra-sensitive shear probe could detect the oceanic turbulence, and then only at dissipation scales (0.01 – 1 m). For this reason, we did not calculate spectra for the *Medusa* velocity data of Tows 3 and 5.

FINDINGS

The following points highlight the principal findings of the measurement program.

- Currents in the eddy exceeded 1.5 m s^{-1} near the surface, and sloping isotherms indicate that currents penetrated to depths greater than 600 meters.

- Turbulence was detected with the shear probes on the towed vehicle. The rate of dissipation of turbulent kinetic energy was typically very small ($\varepsilon < 10^{-8}$ W kg^{-1}). Turbulence was intermittent in space, and occasionally reached up to $\varepsilon = 2 \times 10^{-6}$ W kg^{-1} in the 130 - 150 meter depth range spanning the salinity maxima. These levels of dissipation rate are in keeping with previous scientific studies.

- The water along the tow track was almost always stably stratified, with the exception of a few sections in the surface mixing layer and at greater depth where the buoyancy frequency *N* was very small.

- The eddy sizes (Ozmidov scale, $2 \times L_o$), predicted from the rate of dissipation and the stratification, were quite small. The eddy scale was rarely greater than 1 meter, and only exceeded 4 meters for a few short sections. In these regions the stratification was small, resulting in larger eddy scales.

- Velocity estimates from the *Medusa* ADCP were entirely at the noise level of the instrument (2 cm s^{-1}) rms. Overlap-averaging of the forward beam reduced the noise level to approximately 0.5 cm s^{-1} rms, but failed to reveal environmental signals.

- The velocity scale inferred from the rate of dissipation and the stratification is approximately 1 cm s^{-1}, and is consistent with the measurements made with the ADCP.

- Turbulent velocity fluctuations for the wavenumber range 0.2 to 100 cpm are less than approximately 1 cm s^{-1}, inferred from combining results from the ADCP and shear probe measurements.

ACKNOWLEDGEMENTS

The support and funding provided by the DeepStar consortium are acknowledged, and made this measurement program possible. The support and assistance of the Louisiana Universities Marine Consortium and the superb seamanship of the masters and crew of the *R/V Pelican* are greatly appreciated and were important to the success of the field measurements.

REFERENCES

[1] A. E. Gargett and T. R. Osborn. Small-scale shear measurements during the fine and microstructure experiement (fame). *J. Geophys. Res.*, 86:1929–1944, 1981.

[2] J. O. Hinze. *Turbulence*. McGraw-Hill, New York, 1959.

[3] R. Lueck and T. Osborn. The dissipation of kinetic energy in a warm-core ring. *J.Geophys. Res.*, 91:803–818, 1986.

[4] N. S. Oakey. Determining the rate of dissipation of turbulent kinetic energy from simultaneous temperature and velocity shear microstructure measurements. *J. Phys. Oceanogr.*, 12:256–271, 1982.

[5] G. L. Pickard and W. J. Emery. *Descriptive Physical Oceanography*. Butterworth-Heinemann, Oxford, 1990.

[6} R. Lueck. Deepstar ocean turbulence measurement program. Final report for field work carried out August 23-30, 2003. For Shell International Exploration and Production, Inc. Houston, Texas USA.

TABLE 1: THE TOMI'S SENSOR ARRAY AND THE QUANTITIES MEASURED

Sensor	#	Quantity	Units	Rate(s−1)	Location
Keller Pressure Transducer	1	P P + d*P*/d*t*	dbar	64	Mid-body (internal)
Propeller Current Meter	2	U1 U2	m s^{-1} m s^{-1}	64	Top mast and bottom mast
Linear Servo Accelerometers	3	a_x a_y a_z	m s^{-2}	512	Nose cone (internal)
Angular Rate Gyros	3	ω_x ω_y ω_z	rad s^{-1}	128	Nose cone (internal)
Compass	1	ϕ	rad	64	Pressure Case
Sea-Bird Sensors	3	C T	S m^{-1} ◦C	64	Nose, top mast and bottom mast
Airfoil Shear Probes	2	$\partial w/\partial t$ $\partial v/\partial t$	m s^{-2} m s^{-2}	512	Nose
Thermometrics FP07 Thermistor	2	T T + d*T*/d*t*	◦C	512	Nose

TABLE 2. A SUMMARY OF THE TOWS CARRIED OUT OVER THE COURSE OF THE FIELD WORK. THE SUBSCRIPTS, S, AND, E, DENOTE THE START AND END.

Tow #	Day (Aug.)	$Time_S$ (CDT)	$Time_E$ (CDT)	$Lattitude_S$ (N)	$Longitude_S$ (W)	$Lattitude_E$ (N)	$Longitude_E$ (W)
test1	24	11:26:47	12:45:09	28°51.67′	90°24.36′	28°49.90′	90°27.44′
test2	24	15:30:45	16:03:31	28°48.64′	90°30.96′	28°46.31′	90°28.17′
test3	24	17:05:13	18:30:50	-	-	-	-
1	25-26	18:55:18	19:24:53	28°12.81′	89°44.39′	28°08.54′	89°16.64′
2	27	00:35:24	11:05:56	28°14.88′	89°13.03′	28°23.32′	89°17.03′
3	27	16:15:00	20:21:24	28°31.89′	89°17.27′	28°26.16′	89°09.33′
4	28	02:27:48	11:48:07	28°13.88′	89°45.01′	28°26.64′	89°26.05′
5	28-29	18:39:31	18:47:43	28°13.65′	89°45.07′	28°28.14′	89°28.72′

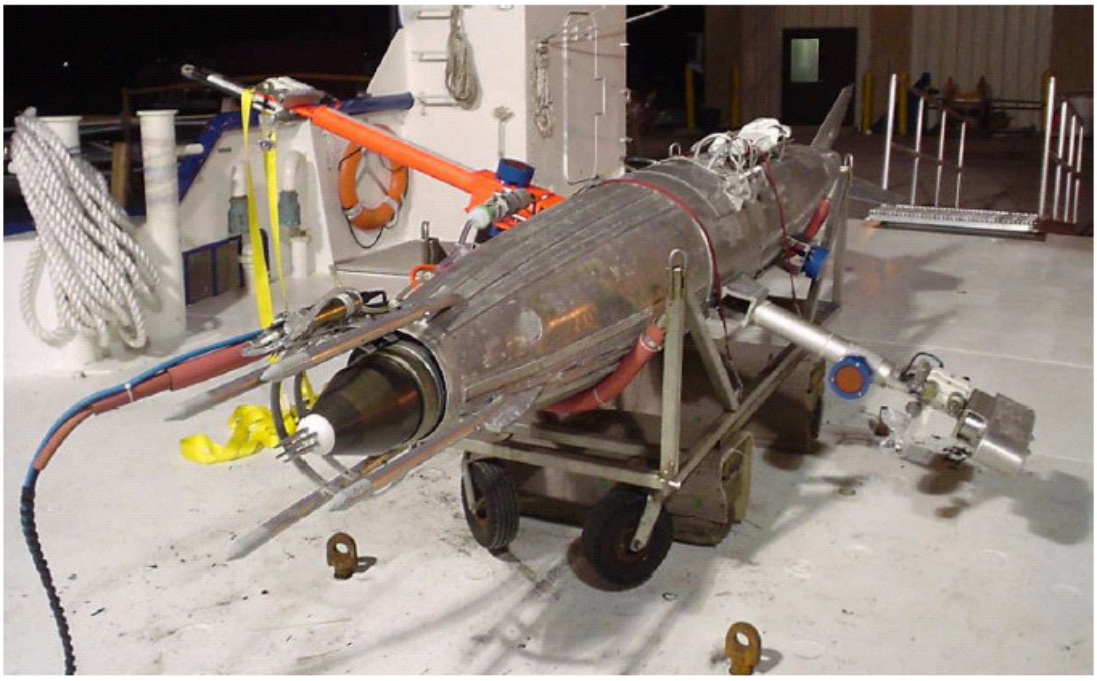

Figure 1. The TOMI on the aft deck of the *R/V Pelican*. The ADCP transducers are mounted on the bottom mast (forward looking), at the base of the (orange) upper mast (port and starboard looking), and behind the lower mast on the main body (downwards looking).

Figure 2. RD Instruments 300 kHz *Medusa* ADCP with 2 meter cables coupling the instrument to its four transducers.

Ship–mounted ADCP data collected en route to Europa, 24 Aug. 2003
Average velocity in the top 50m

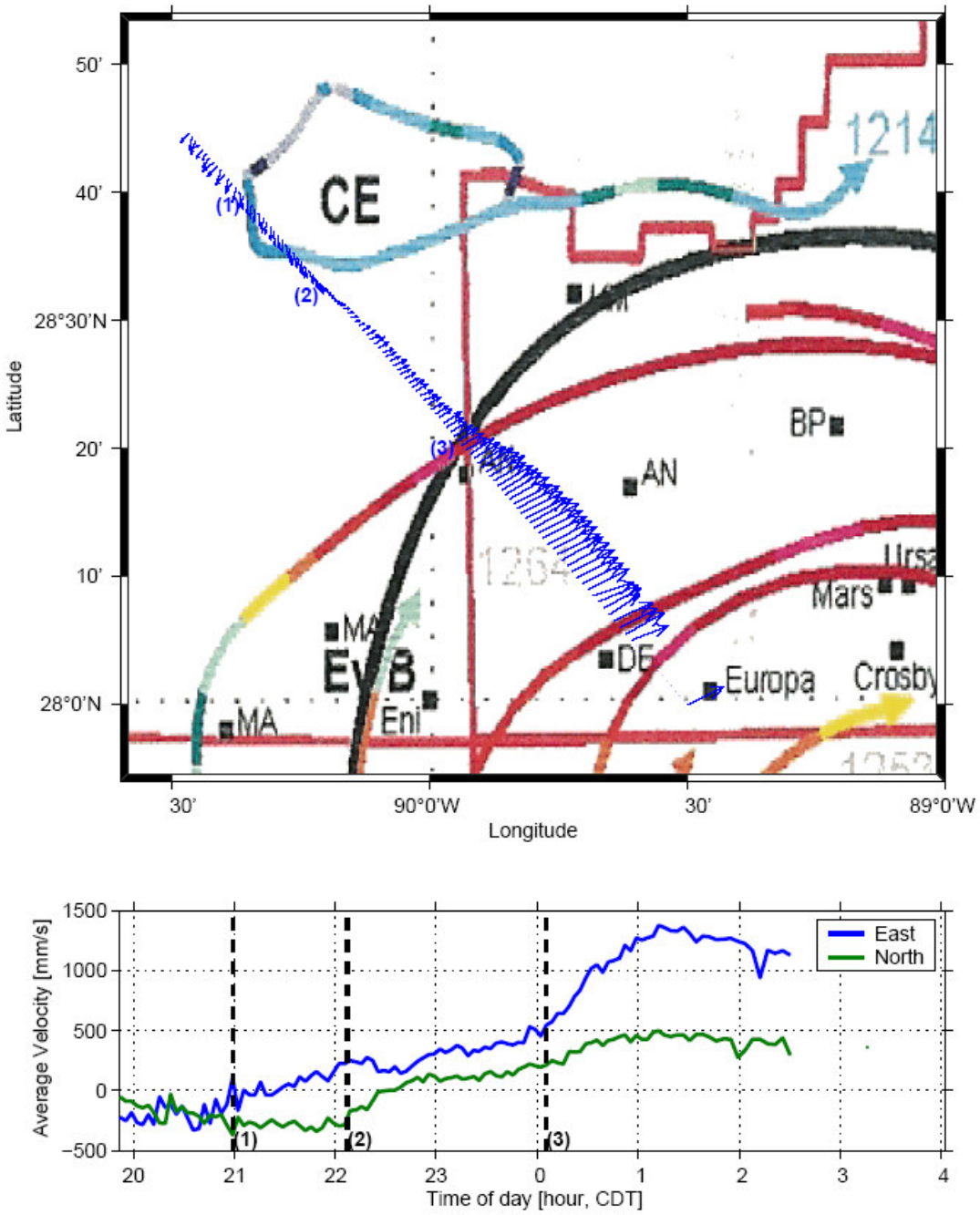

Figure 3. The upper panel is a stick plot depicting the average current velocity and direction from the surface to 50 meters depth (11 bins), as measured by the shipboard 75 Hz ADCP. The vectors have been temporally averaged over 50 pings (about 200 seconds). The background is the EddyWatch map. The red lines are drifting buoy tracks. The lower panel shows the same velocity vectors decomposed into the north and east components and plotted as a time series.

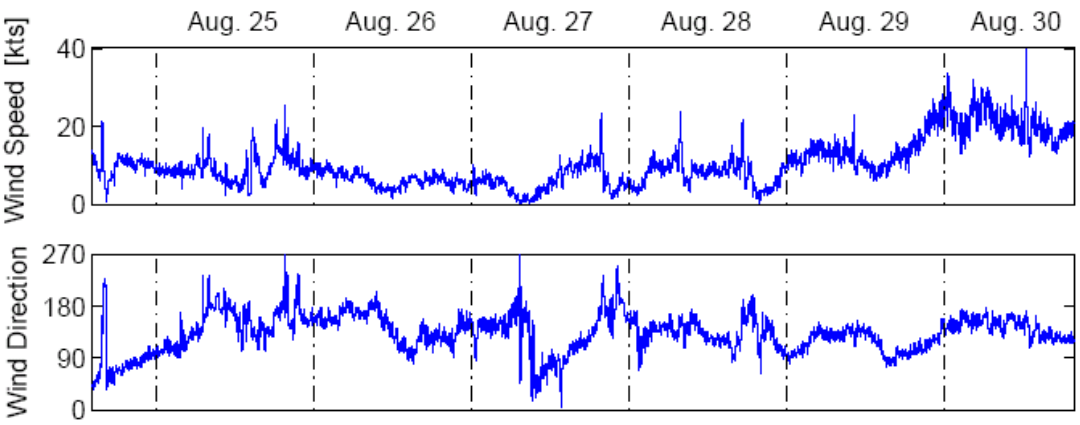

Figure 4. Meteorological data collected using the shipboard MIDAS system (August 24-30). From top down, the quantities displayed are true wind speed and wind direction.

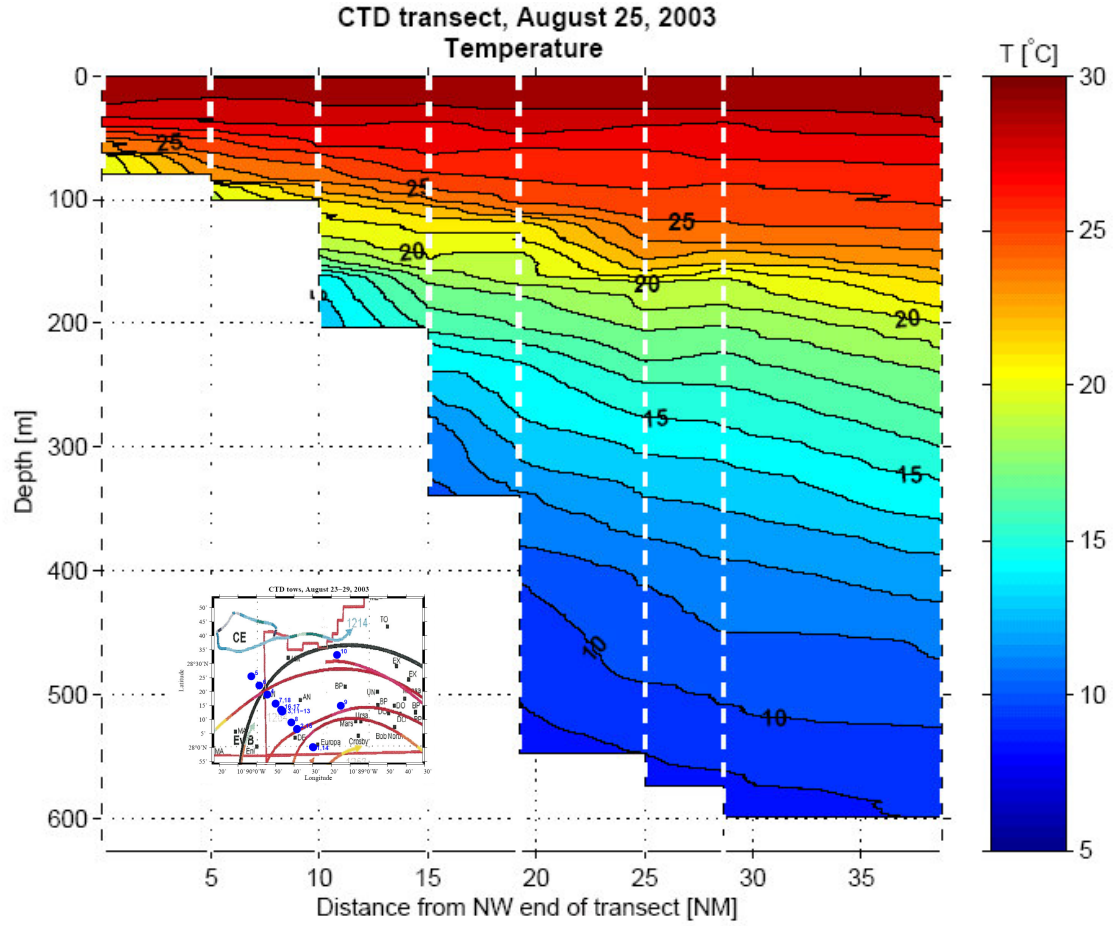

Figure 5. A cross-section of temperature generated from the CTD casts, the locations of which are shown in the inset.

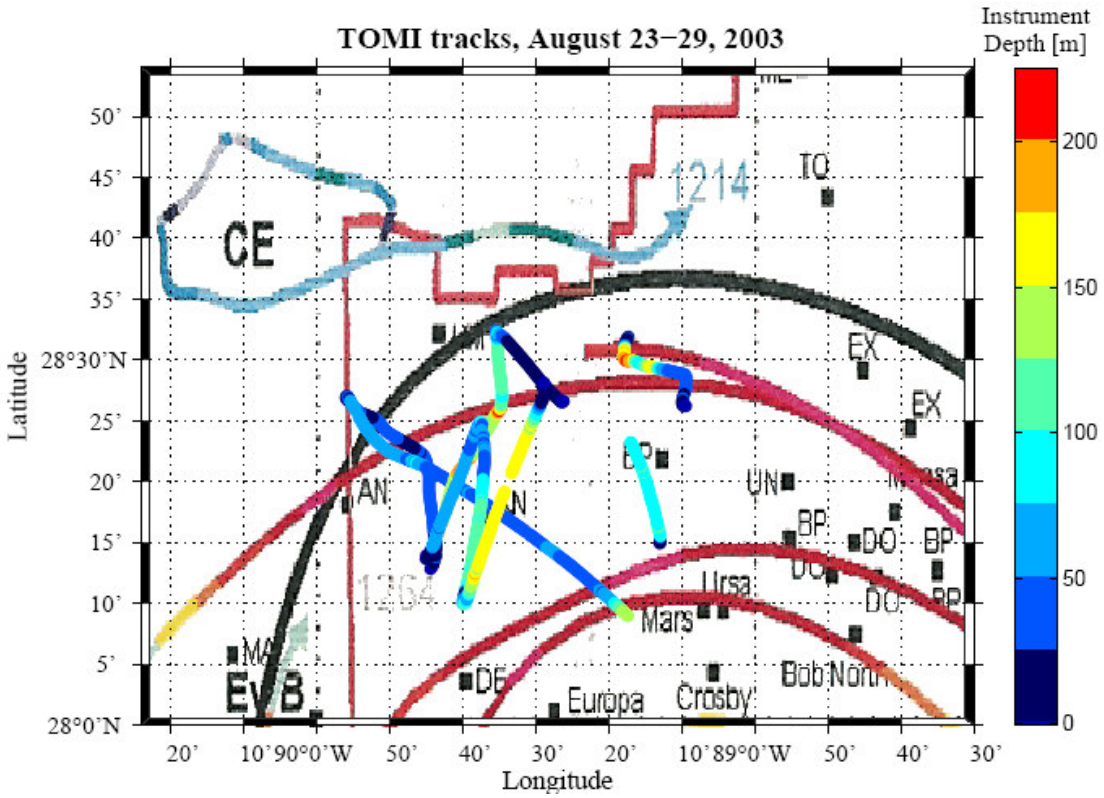

Figure 6. The track and depth profiles for all tows, superimposed on the position of the eddy as described by the EddyWatch map. The depth of the towed vehicle is revealed by the color of the tow track. The tow numbers are not shown, but each tow has a unique shape and is easily identified by reference to Figure 7. The heavy black curve shows the location of the eddy front predicted by the Eddy Watch map of August 14-21, 2003.

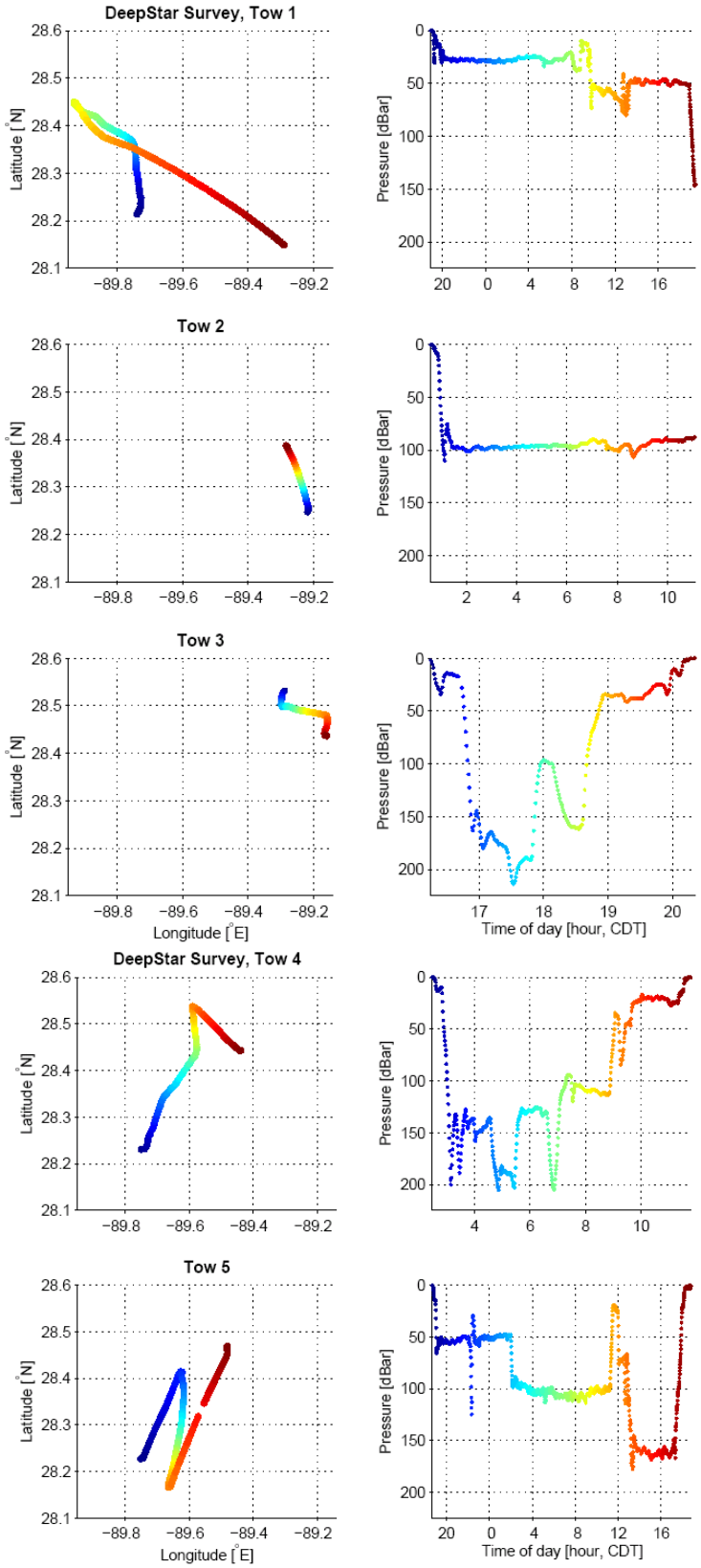

Figure 7. The track and depth profiles for all five TOMI tows (Aug 25-29).

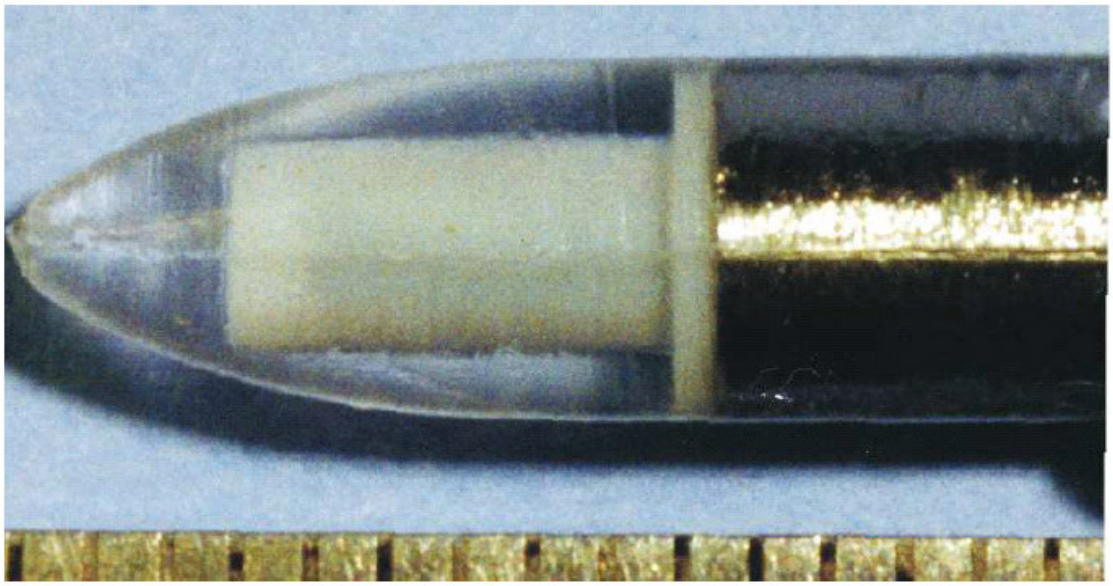

Figure 8. A photograph of the airfoil shear probe. The piezo-ceramic beam is encased in a teflon mantle (white center), which itself is molded in silicon rubber to give the probe its characteristic axi-symmetric profile. The increments on the ruler at the bottom are 1 mm.

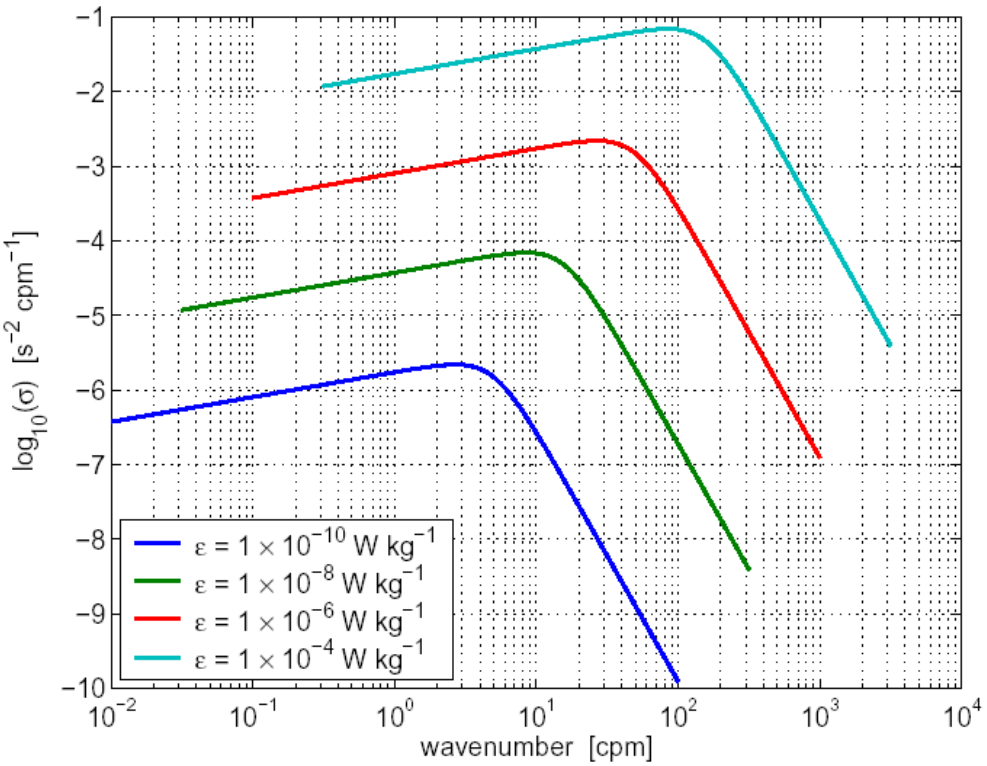

Figure 9. The hypothetical true shear spectrum for dissipation rates of 1×10^{-10}, 1×10^{-8}, 1×10^{-6} and 1×10^{-4} W kg^{-1}.

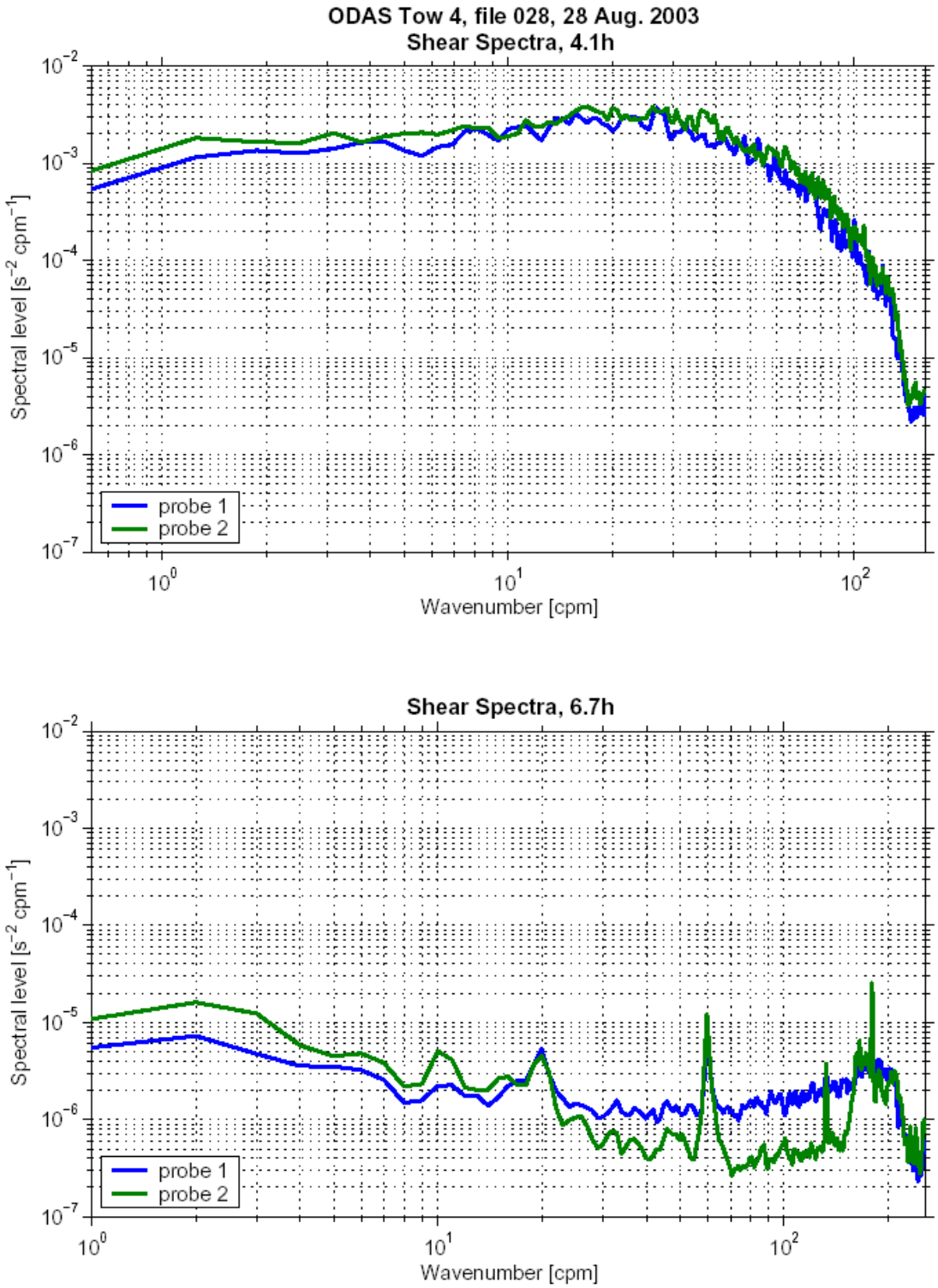

Figure 10. Examples of shear spectra with respect to wavenumber from Tow 4, for a region of high shear where $\varepsilon = 2 \times 10^{-6}$ W kg^{-1} (top panel), and a region of lower shear where $\varepsilon = 3 \times 10^{-10}$ W kg^{-1} (lower panel).

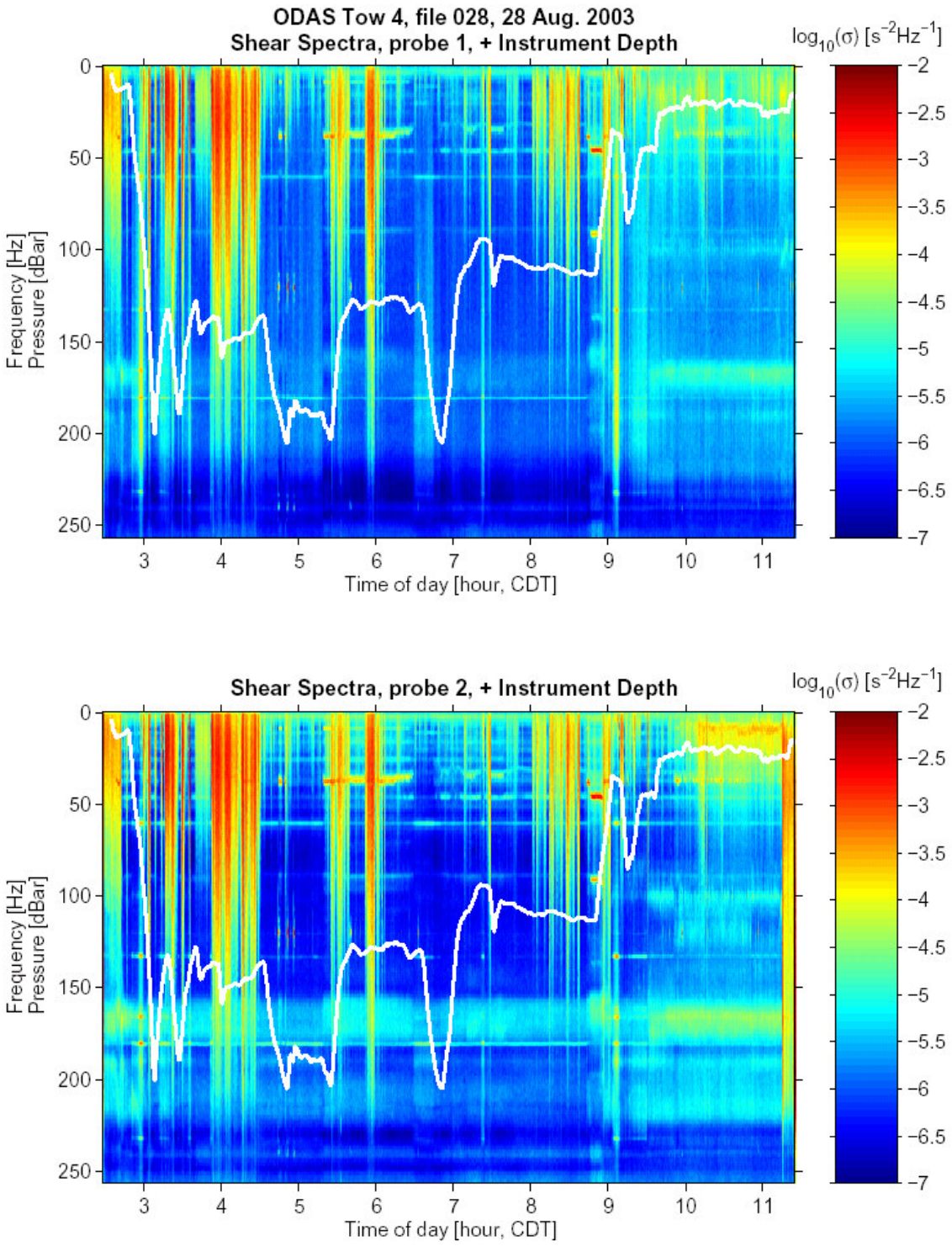

Figure 11. Shear spectra from two airfoil probes for Tow 4. The frequency is plotted on the y-axis, and time is relative to the x-axis. The depth profile is superimposed on the spectral levels to provide insight into spectral variability relative to depth. The Eddy Front was touched at 0900 CDT.

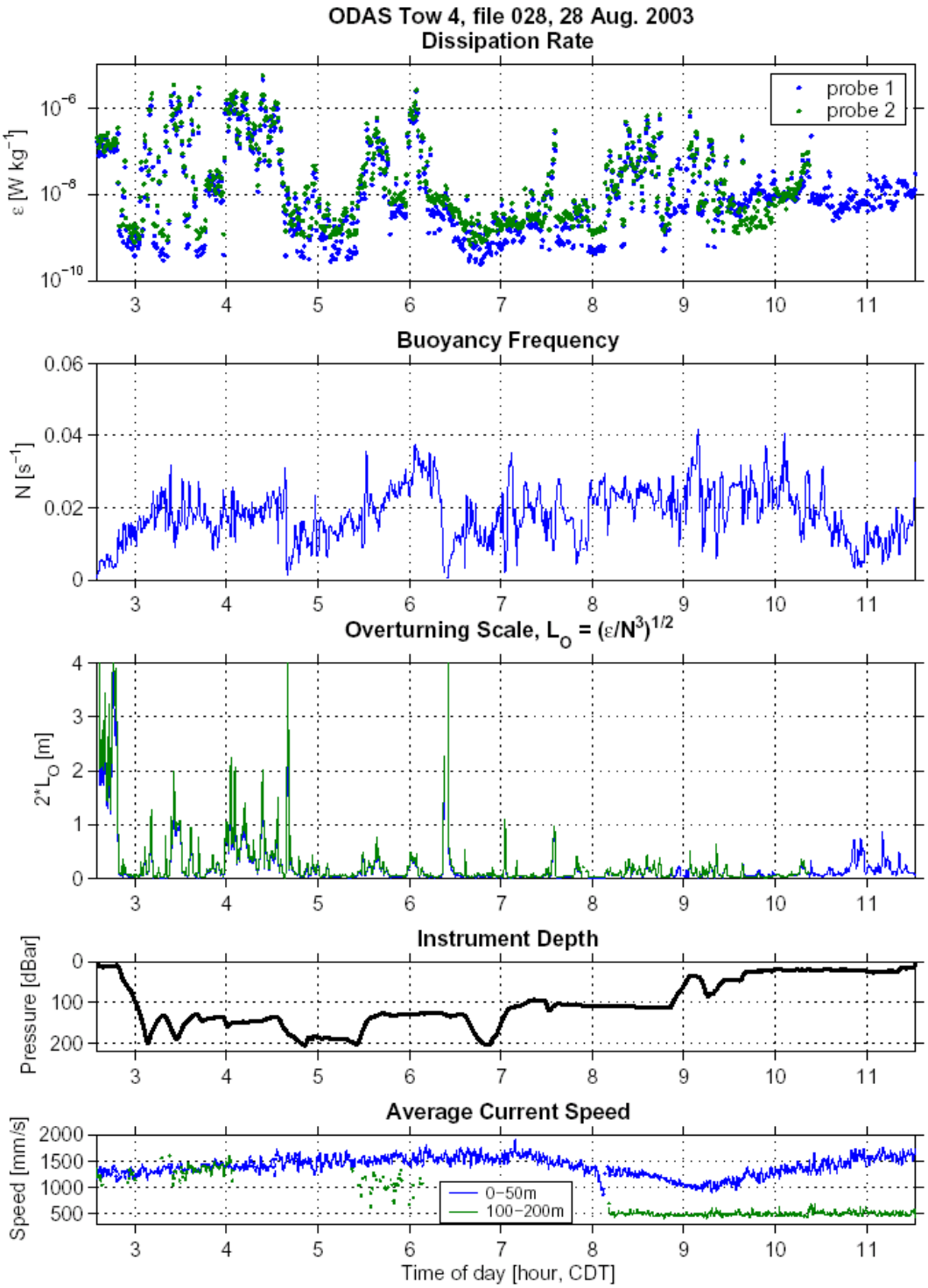

Figure 12. From top to bottom panel, respectively; the rate of dissipation (ε), buoyancy frequency (*N*), and Ozmidov length scale ($2\times L_o$), vehicle depth, and current speed derived from the 75 kHz ADCP for Tow 4 (Aug. 28). The current speed is derived from the vector averaged velocity between the surface and 50 m depth, and between 100 and 200 m depth. The vectors were also time averaged over 200 seconds (50 pings). The eddy front is at 0900 hours.

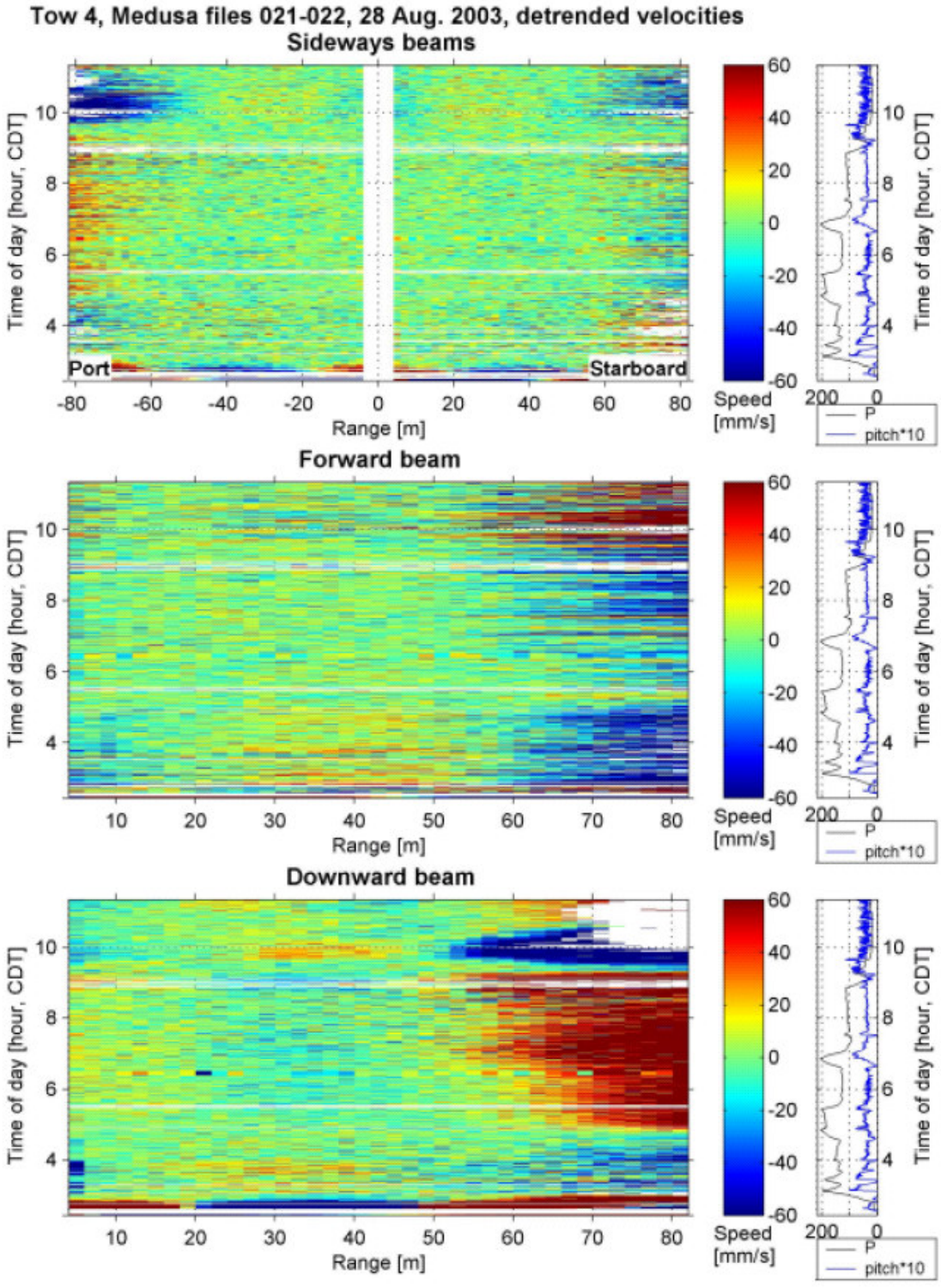

Figure 13. De-trended velocity estimates from the sideways, forwards and downwards looking transducers (Tow 4).

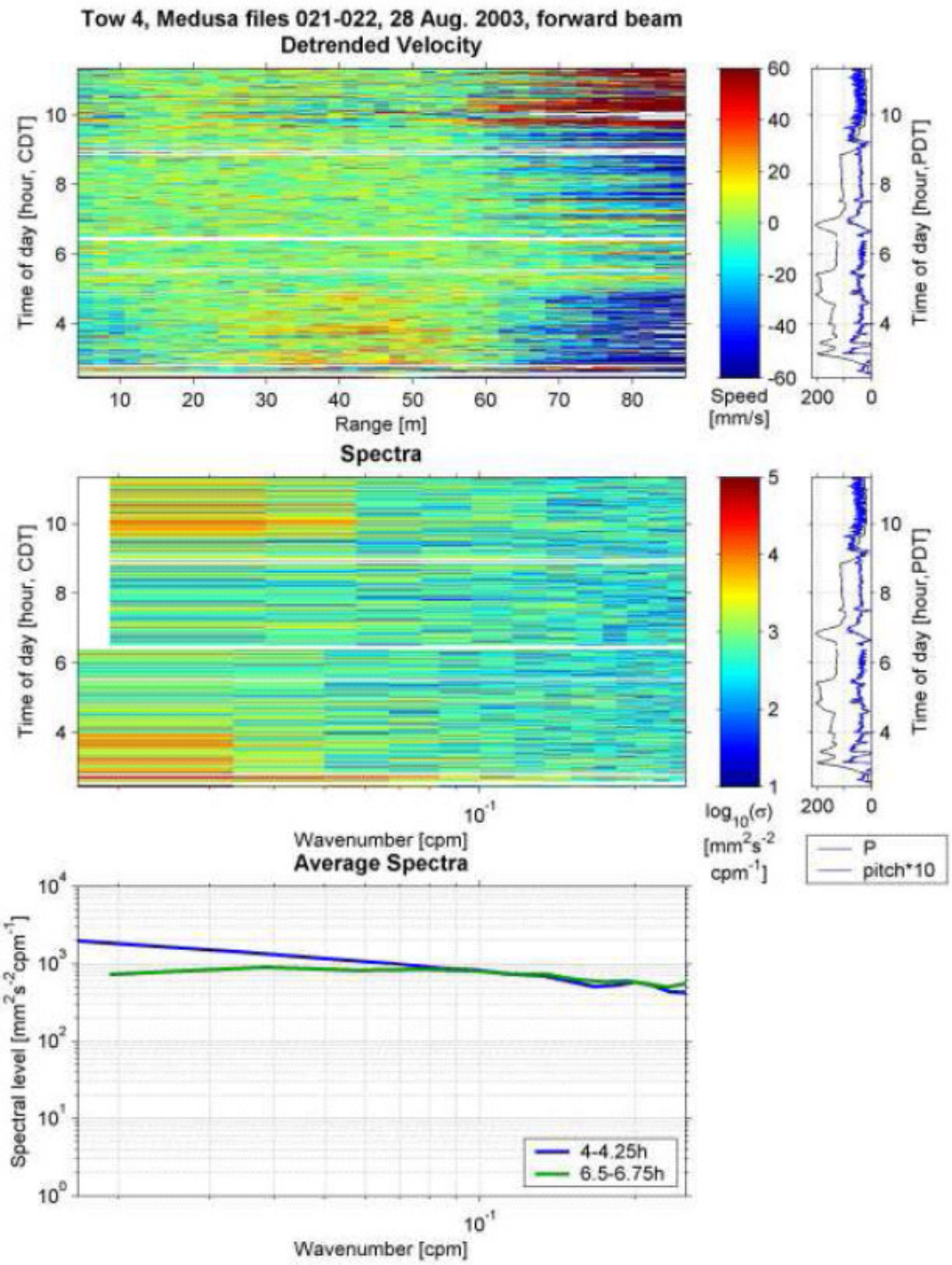

Figure 14. De-trended velocity estimates from the forward looking beam for Tow 4 (top panel), velocity spectra with respect to wavenumber (middle panel), and examples of forward beam velocity spectra from a turbulent period (4-4.25h, ε = 1 × 10–6 W kg^{-1}), and a fairly non-turbulent period (6.5-6.75h, ε = 2 × 10–9 W kg^{-1}). The tick marks along the horizontal axis have integer steps with the left-most at 2×10^{-2} the next at 3×10^{-2} and the right most tick mark at 20 × 10^{-1}.

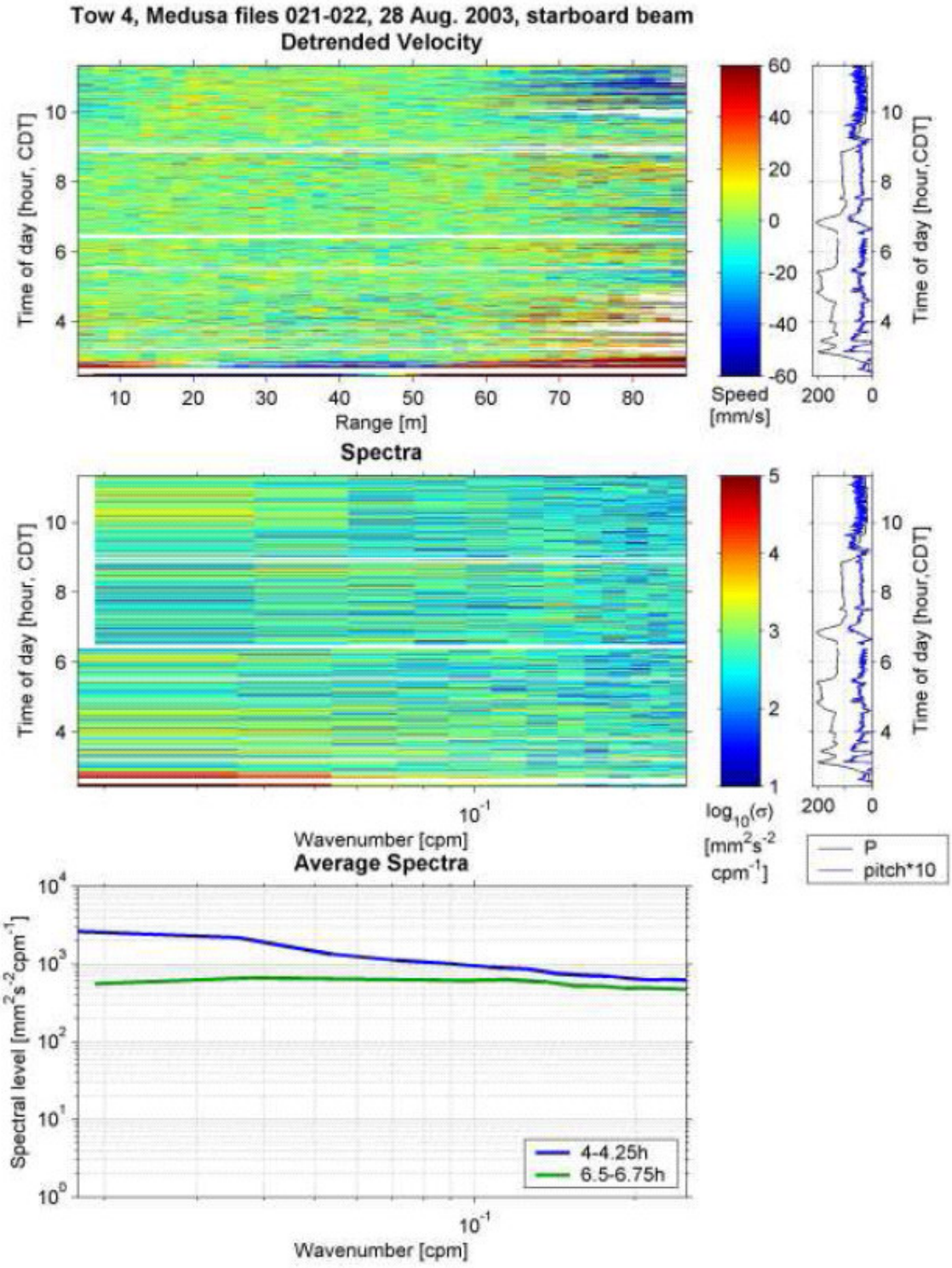

Figure 15. De-trended velocity estimates from the starboard looking beam for Tow 4 (top panel), velocity spectra with respect to wavenumber (middle panel), and examples of starboard beam velocity spectra from the same two periods plotted in the bottom panel of Figure 14. The tick marks along the horizontal axis have integer steps with the left-most at 2×10^{-2} the next at 3×10^{-2} and the right most tick mark at 20×10^{-1}.

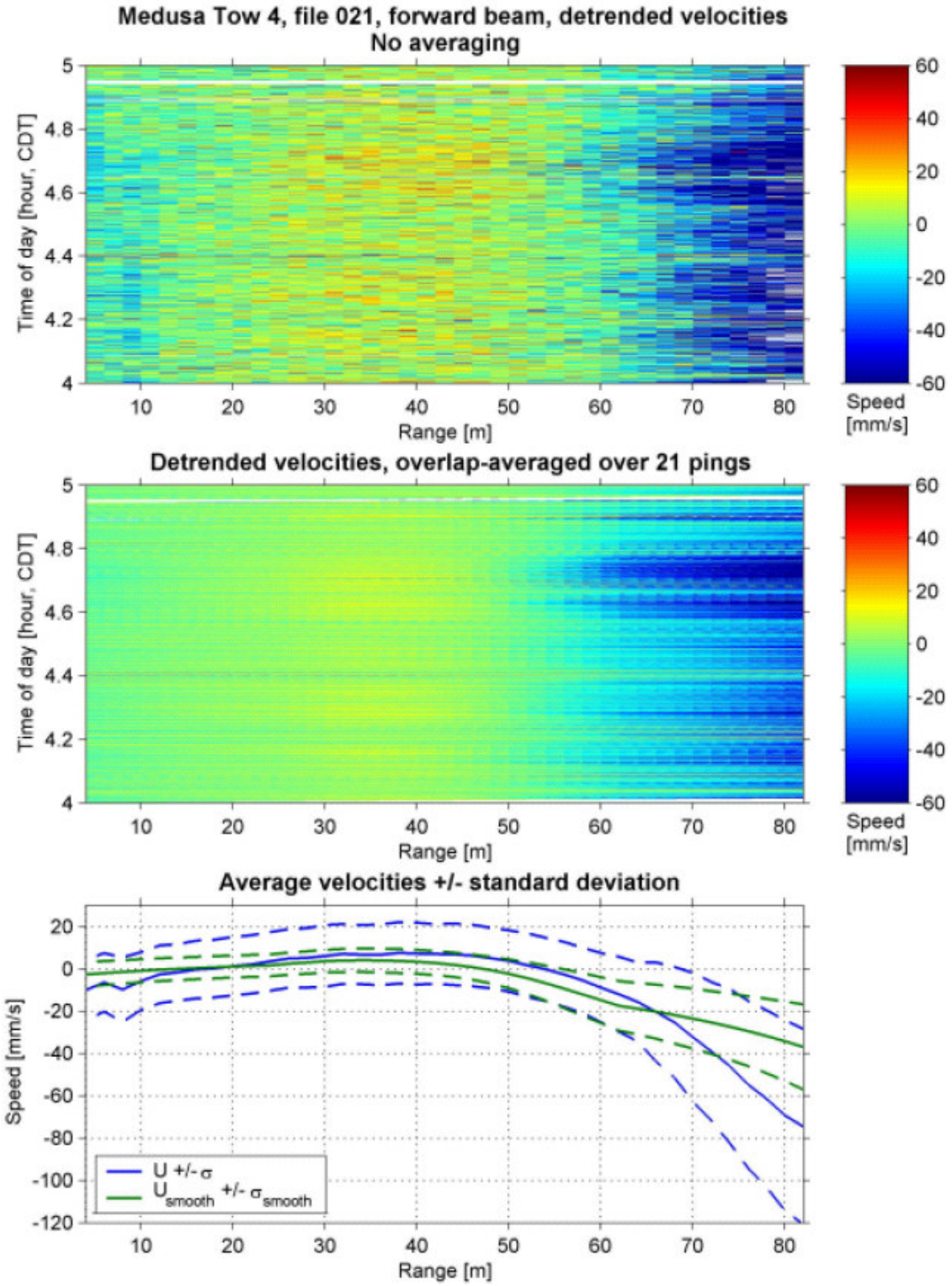

Figure 16. De-trended (top panel) and overlap-averaged (middle panel) velocity estimates from the forward beam, and their means and standard deviations before (blue lines) and after (green lines) overlap-averaging over 21 pings (bottom panel).

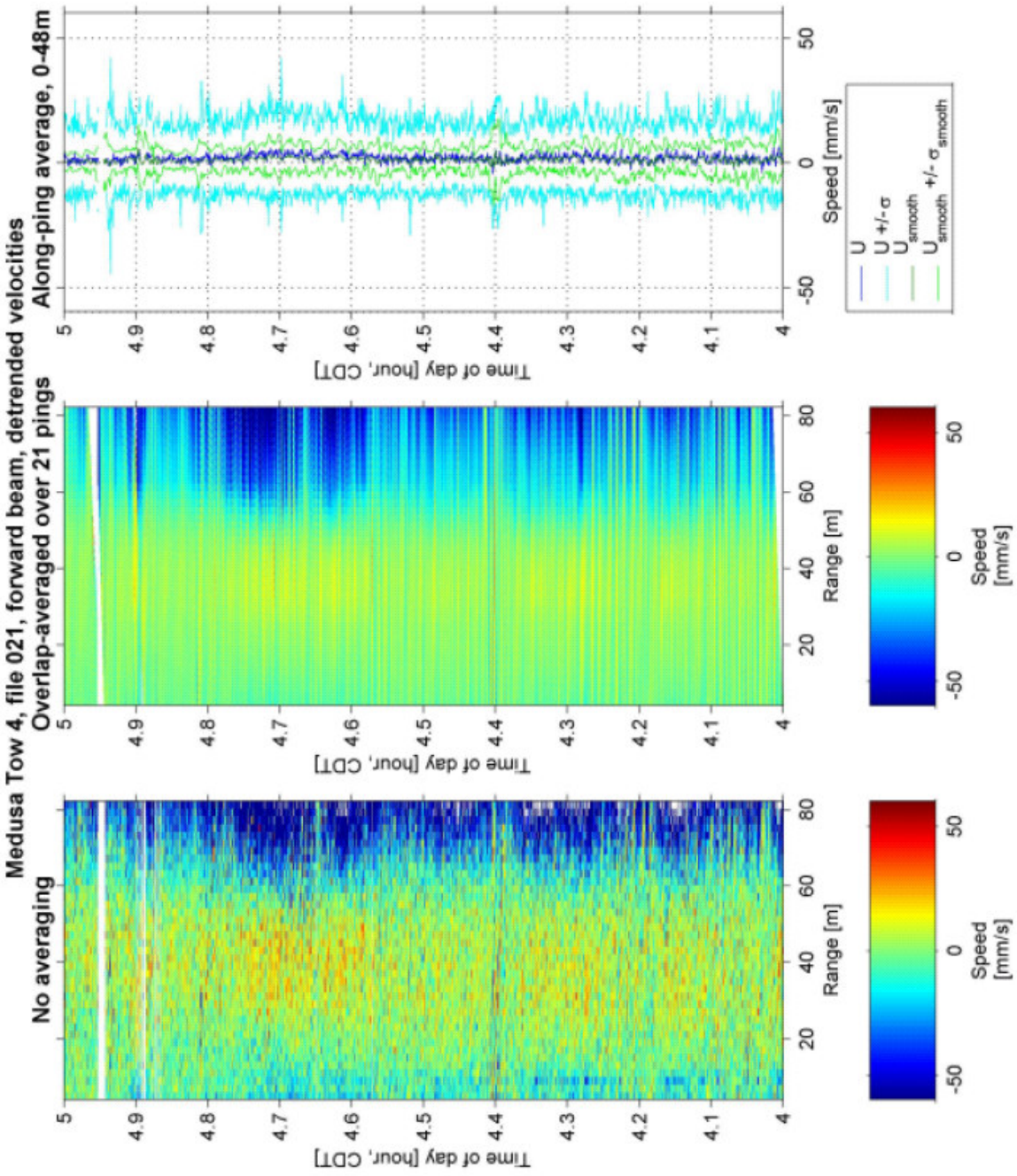

Figure 17. View as landscape. De-trended (left panel) and overlap-averaged (middle panel) velocity estimates from the forward beam, and their means and standard deviations before and after averaging along pings (right panel).

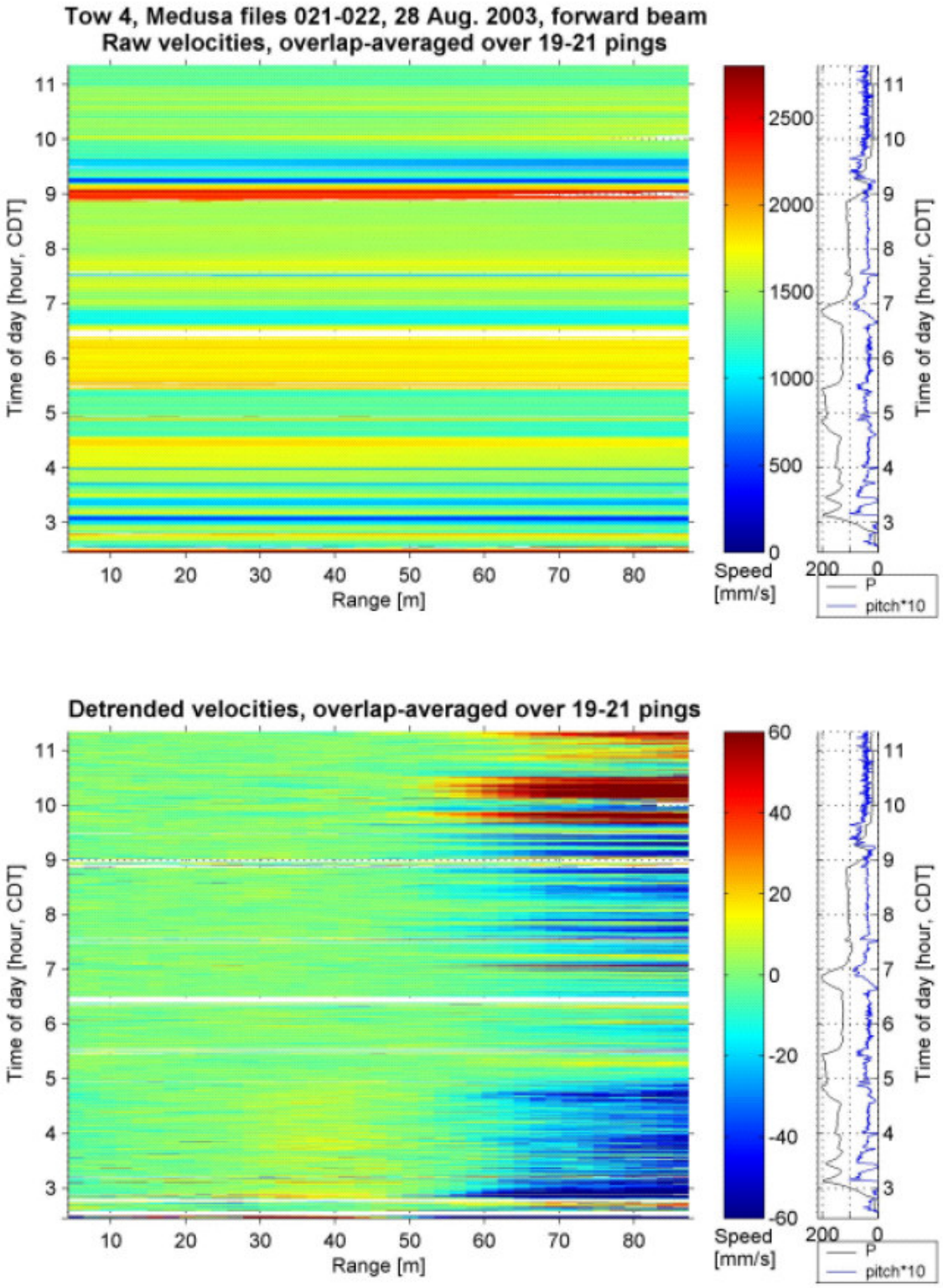

Figure 18. Raw (top panel) and de-trended (bottom panel) velocity estimates from the forward beam (Tow 4) after overlap-averaging (19 - 21 pings). The large variations in color in the upper panel reflect the variations in tow speed.

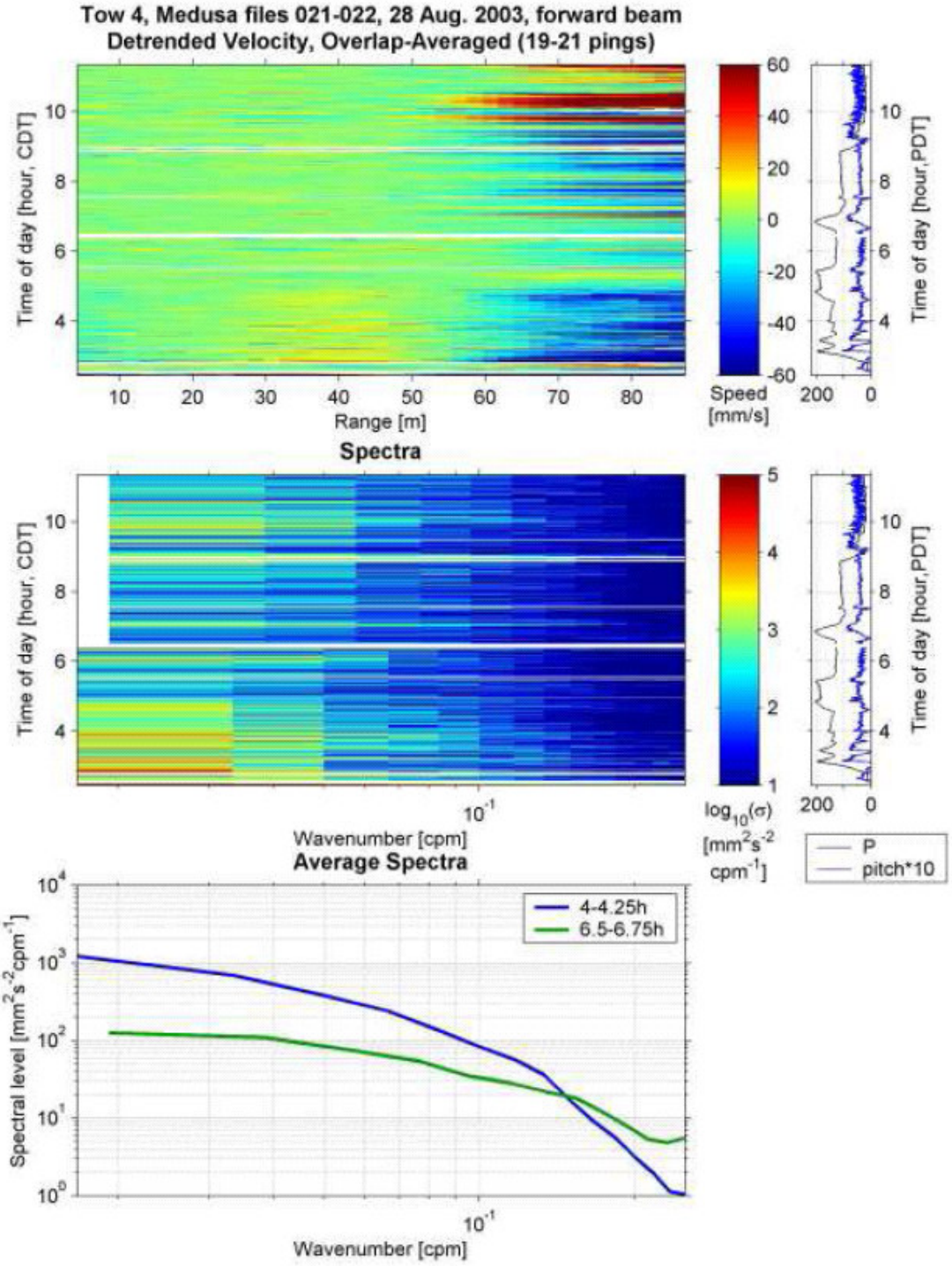

Figure 19. Overlap-averaged, de-trended velocity estimates from the forward beam (Tow 4), velocity spectra with respect to wavenumber (middle panel), and the overlap-averaged versions of the line spectra shown in Figure 14 (bottom panel). The standard deviation for hours 4 to 4.25h and 6.5 to 6.75 are σ = 7.9 mm s^{-1} and σ = 3.2 mm s^{-1} respectively. The tick marks along the horizontal axis have integer steps with the left-most at 2 × 10^{-2} the next at 3 × 10^{-2} and the right most tick mark at 20 × 10^{-1}.